Determination of intramolecular isotope distribution of ozone by oxidation reaction with silver metal

S. K. Bhattacharya, A. Pandey, Joel Savarino

Determination of intramolecular isotope distribution of ozone by oxidation reaction with silver metal

S. K. Bhattacharya,[1] Antra Pandey,[1] and J. Savarino[2]

Received 4 December 2006; revised 29 August 2007; accepted 18 October 2007; published 9 February 2008.

[1] The intramolecular distribution of ^{17}O in ozone was determined by a new technique using oxidation reaction of ozone with silver and measuring the isotope ratios $^{18}O/^{16}O$ and $^{17}O/^{16}O$ of silver oxide, ozone and leftover oxygen. These data along with known ^{18}O distribution in ozone given by Janssen (2005) in terms of $r^{50} = [^{16}O^{16}O^{18}O]/[^{16}O^{18}O^{16}O]$ allow us to determine $r^{49} = [^{16}O^{16}O^{17}O]/[^{16}O^{17}O^{16}O]$. It is seen that r^{49} values increase from 2.030 to 2.145 with increase of bulk ^{17}O enrichment in ozone from 11.7‰ to 106.3‰ (controlled by varying temperature and pressure during ozone formation) just as r^{50} values increase from 1.922 to 2.089 with increase in bulk ^{18}O enrichment over the same range. Over bulk enrichment level up to ~100‰ the r^{49} values are higher than r^{50} values by 0.075 ± 0.026. The difference is small but significant since it corresponds to a large change in enrichment values of the asymmetric and symmetric types of $^{17}O^{16}O_2$ and $^{18}O^{16}O_2$ relative to a hypothetical ozone standard with statistical isotope distribution. The difference reduces with increase in bulk ozone enrichment. We do not find any significant variation in r values between ozone samples made by Tesla discharge and by UV photolysis of oxygen. Additionally, for ozone samples with negligible enrichment, the symmetrical isotopomers have relatively more heavy isotopes than the asymmetrical ones consistent with their bond strength difference. Atmospheric implications of the results are briefly discussed.

Citation: Bhattacharya, S. K., A. Pandey, and J. Savarino (2008), Determination of intramolecular isotope distribution of ozone by oxidation reaction with silver metal, *J. Geophys. Res.*, *113*, D03303, doi:10.1029/2006JD008309.

1. Introduction

[2] Stratospheric and tropospheric ozone [*Rinsland et al.*, 1985; *Abbas et al.*, 1987; *Mauersberger*, 1987; *Mauersberger et al.*, 2001; *Schueler et al.*, 1990; *Krankowsky et al.*, 1995; *Meier and Notholt*, 1996; *Irion et al.*, 1996; *Johnston and Thiemens*, 1997; *Lämmerzahl et al.*, 2002] and laboratory-made ozone [*Thiemens and Heidenreich*, 1983; *Thiemens and Jackson*, 1987, 1988; *Morton et al.*, 1990; *Bhattacharya et al.*, 2002] have unusual propensity of heavy isotopes ^{17}O and ^{18}O relative to the parent molecular oxygen reservoir from which it is formed. The isotopic ratios in an ozone sample are usually expressed in terms of delta values defined as (for ^{17}O),

$$\delta^{17}O = \left[\left(^{17}O/^{16}O\right)_{\text{sample}} / \left(^{17}O/^{16}O\right)_{\text{reference}}\right] - 1 \times 10^3 \left(\text{in per mill or } ‰\right) \quad (1)$$

where "reference" denotes the reservoir for comparison. $\delta^{18}O$ is also defined in the same way. In ozone formed near atmospheric conditions, both ^{17}O and ^{18}O are enriched by ~100‰ and surprisingly, $\delta^{17}O$ is not half of $\delta^{18}O$ as expected for normal mass-dependent fractionation process. Being a triangular molecule, a heavy isotopologue of ozone like $^{18}O^{16}O_2$ can have the ^{18}O isotope located either at the central (apex) position ($^{16}O^{18}O^{16}O$ with C_{2v} symmetry) or at the terminal (base) position ($^{16}O^{16}O^{18}O$ with C_s symmetry). Statistically, C_s or asymmetric type of ozone is expected to be exactly twice more abundant compared to C_{2v} or symmetric type of ozone and thus their ratio $r^{50} = [^{16}O^{16}O^{18}O]/[^{16}O^{18}O^{16}O]$ should be equal to two if no isotopic discrimination takes place. Since for a given bulk ^{18}O enrichment ($\delta^{50}_{\text{bulk}}O_3 = \delta^{18}_{b}O$) the terminal position and central position enrichments are connected with the abundance of asymmetric molecules and symmetric molecules (relative to their statistical abundances) respectively, the ratio r^{50} can simply be expressed in terms of enrichments in asymmetric ($\delta^{50}_{a}O_3 = \delta^{18}_{a}O$) and symmetric ($\delta^{50}_{s}O_3 = \delta^{18}_{s}O$) ozone which are defined here in terms of relative deviation of the abundance ratio $[^{18}O]/[^{16}O]$ in symmetric or asymmetric species from the abundance ratio based on the simple statistical distribution. For practical purpose, the hypothetical statistical distribution of isotopes in the ozone molecule is defined with reference to the molecular oxygen in the following way. If the elemental isotope ratio $[^{18}O]/[^{16}O] = f$, the statistical distribution is obeyed when in molecular oxygen species we get $[^{18}O^{16}O]/[^{16}O^{16}O] = 2f$, and in asymmetric and symmetric ozone

[1]Physical Research Laboratory, Ahmedabad, India.
[2]Laboratoire de Glaciologie et Géophysique de l'Environnement, Centre National de la Recherche Scientifique, Université Joseph Fourier-Grenoble, Saint Martin d'Heres, France.

0148-0227/08/2006JD008309

species we get $[^{18}O^{16}O^{16}O]/[^{16}O^{16}O^{16}O] = 2f$ and $[^{16}O^{18}O^{16}O]/[^{16}O^{16}O^{16}O] = f$ respectively. If, for a given ozone sample made from a particular tank oxygen, the observed isotopomer ratios do not obey the above rule, we characterize it as enrichment or depletion relative to the statistical distribution. The deviation from statistical distribution of isotopes in ozone molecules is experimentally obtained by converting a given ozone sample to molecular oxygen and analyzing it with reference to the tank molecular oxygen from which it was made. It follows that (where δ values are expressed in ‰):

$$r^{50} = 2\left(1 + 10^{-3} \times \delta_a^{18}O\right)/\left(1 + 10^{3} \times \delta_s^{18}O\right) \quad (2)$$

[3] The statistical ratio $r^{50} = 2$ is possible only if enrichments or depletions expressed by $\delta_a^{18}O$ and $\delta_s^{18}O$ are equal or in particular, both are zero.

[4] Experimental evidences have demonstrated that the statistical rule is violated in case of highly enriched ozone (>60‰) made in the laboratory [*Anderson et al.*, 1989; *Larsen and Pedersen*, 1994; *Larsen et al.*, 2000; *Janssen*, 2005] where the asymmetric species is more abundant than expected from simple statistics. The isotopomeric distribution of ^{18}O in heavy ozone was first studied by *Anderson et al.* [1989] using infrared tunable diode laser absorption spectroscopy (TDLAS) but with a large error in the measurement. Later, *Larsen and Pedersen* [1994] and *Larsen et al.* [2000] applied Fourier transform IR spectroscopy (FTIRS) technique to determine r^{50}. Large uncertainties are associated with the spectroscopic techniques due to experimental limitations and uncertain line strength information. Nevertheless, both TDLAS and FTIRS study showed that for $^{18}O^{16}O_2$ species $r^{50} > 2$. In a recent review, *Janssen* [2005] has summarized all the earlier experimental results and conclude that for bulk ozone if $\delta_b^{18}O > 60‰$, $r^{50} > 2$. He also showed that both $\delta_a^{18}O$ and $\delta_s^{17}O$ are positive; that is, the bulk enrichment is not exclusively due to the asymmetric species but also contributed by symmetric species. An apparent contradiction was noted in the FTIRS study of *Larsen et al.* [2000] who reported a ratio $r^{50} = 1.99 \pm 0.04$ for the level of enrichment where the TDLAS study gave a value of 2.128 ± 0.028. However, this discrepancy was resolved by *Janssen* [2005] by invoking temperature dependence of isotopic enrichment and associated r^{50} value. On the basis of this compilation Janssen concluded that the ratio r^{50} is mostly different from 2.00 and increases from 1.99 to 2.14 when the bulk ozone enrichment increases from 47‰ to 156‰.

[5] The departure of r^{50} from the statistical value of two (i.e., $r^{50} > 2$) is related to the variation in the rate of formation of various ozone isotopomers arising out of combination of isotopes involved in $O + O_2$ collision [*Anderson et al.*, 1997; *Janssen et al.*, 1999, 2001]. For example, $^{16}O^{16}O^{18}O$ can result from collision of ^{16}O with $^{16}O^{18}O$ or collision of ^{18}O with $^{16}O^{16}O$ but the rates are very different (1.45 and 0.92 respectively when expressed relative to the rate of $^{16}O + {}^{16}O^{16}O \rightarrow {}^{16}O^{16}O^{16}O$) [*Janssen et al.*, 2001]. Similarly, $^{16}O^{16}O^{18}O$ and $^{16}O^{18}O^{16}O$ have different rates of formation though both can be produced from collision of ^{16}O with $^{16}O^{18}O$. *Janssen et al.* [2001] showed that in case of homonuclear oxygen molecules the relative rate coefficient of a given ozone formation reaction shows a linear correlation with the enthalpy (or change in zero point energy) of the associated exchange reaction. It seems that when exchange of an oxygen isotope with an oxygen molecule has an energy barrier, there is increased probability of ozone formation in the corresponding channel. This led *Janssen et al.* [2001] to propose that endothermic exchange corresponds to longer lifetime of the collision complex resulting in a higher recombination rate with the same isotopic partners.

[6] Using the above results, a phenomenological theory was proposed by Marcus and coworkers to explain the rate coefficient variation among isotopic partners in ozone formation process. The proposal is based on a modification of the RRKM theory of unimolecular dissociation which takes into account reduction in density of states due to limitation in mode coupling or nonrandomness [*Hathorn and Marcus*, 1999, 2000; *Gao and Marcus*, 2001, 2002]. They proposed that asymmetric reaction intermediate formed in $O+O_2$ collision has a relatively larger density of states (permitting enhanced randomness and longer lifetime than that of symmetric reaction intermediate) which results in its more efficient quenching to ground state ozone. Because of this non-RRKM effect the enrichment in the symmetric and asymmetric types of ozone would differ. In other words, the terminal and central position in the ozone molecule should have different isotopic enrichment and one would expect an intramolecular isotopic variation resulting in ratio $r^{50} > 2$.

[7] As of now, there is no study on internal distribution of ^{17}O in ozone isotopologue $^{17}O^{16}O_2$ due to comparatively larger difficulties in spectroscopic measurement owing to its smaller abundance. We may mention here that in their recent work Janssen and Tuzson [*Janssen and Tuzson*, 2006; *Tuzson and Janssen*, 2006; *Tuzson*, 2005] attempted to establish a new TDLAS technique to provide data on the internal distribution of both ^{17}O and ^{18}O. However, for reasons explained in section 3.3 we use only *Janssen*'s [2005] compilation of r^{50} for the present work and show how one can determine the values of r^{49} using this compilation.

[8] *Sheppard and Walker* [1983] showed in a theoretical study that in ozone dissociation by photons a terminal atom is emitted more than 90% of the time. It is also believed that the high oxidative reactivity of ozone is due to the relative ease with which the terminal atoms can react with other atoms compared to the central atom. If this is true then it is possible to determine the intramolecular isotope distribution in ozone by chemical reaction method. For example, it is known that ozone reacts with silver foil at an extremely fast rate forming silver oxide as a thin layer (see *Waterhouse et al.* [2001, 2002] for details and earlier references). We made use of this reaction as a chemical probe to study the internal isotope distribution of ^{17}O in ozone by characterizing the isotope transfer. The advantage of this method is that it does not involve the formation of O atom and thus there is no possibility of oxygen isotope exchange with the reactant and molecular oxygen as happens in case of O_3-CO reaction [*Bhattacharya and Thiemens*, 1989; *Pandey and Bhattacharya*, 2006] or O_3-CO_2 exchange reaction [*Wen and Thiemens*, 1993; *Chakraborty and Bhattacharya*, 2003; *Shaheen et al.*, 2007] via involvement of $O(^1D)$. The isotopic composition of the reacting ozone and the oxygen

Table 1. Comparison of the Oxygen Isotopic Compositions of Ozone Obtained From Mass Balance Calculation, $\delta(\text{ozone}) \times [O_2(Ag_2O) + O_2(\text{leftover})] = \delta(Ag_2O) \times [O_2(Ag_2O)] + \delta(O_2\ (\text{leftover})) \times [O_2(\text{leftover})]$, and From Direct Measurement by Aliquot Method[a]

	Ag_2O			Leftover O_2			Ozone (Mass Balance)			Ozone (Measured)	
Sample	Amount, μmol	$\delta^{18}O$	$\delta^{17}O$	Amount, μmol	$\delta^{18}O$	$\delta^{17}O$	Amount, μmol	$\delta_b^{18}O$	$\delta_b^{17}O$	$\delta_b^{18}O$	$\delta_b^{17}O$
L-1	11	−1.4	17.4	73	12.5	10.8	84	10.7	11.7	12.3	12.7
L-2	8	5	25.8	50	23.2	21.0	58	20.7	21.7	23.2	23.7
L-3	5	19.4	36.6	120	28.4	28.7	125	28.1	29.0	29.9	30.2
L-4	10	26.0	45.5	89	40.9	39.8	99	39.4	40.4	40.8	41.7
L-5	4	35.4	52.1	35	47.1	44.6	39	45.9	45.4	42.3	44.4
L-6	10	42.1	58.2	74	37.6	31.3	84	52.3	51.6	52.3	51.6
L-7	5	38.7	56.1	22	56.4	50.2	27	53.1	51.2	52.3	52.6
L-8	3	58.2	66.3	115	60.7	56.8	118	60.7	57.1	58.3	55.6
L-9	9	56.7	70.4	89	65.2	59.3	98	64.4	60.3	67.6	62.6
L-10	9	72.6	82.2	117	76.7	69.5	126	76.4	70.4	77.7	71.1
L-11	12	76.5	85.9	98	84.8	74.2	110	83.9	75.4	86.2	77.3
L-12	6	81.0	88.5	78	84.3	75.7	84	84.1	76.6	87.8	78.6
L-13	3	88.0	88.2	44	86.2	76.0	47	86.4	76.8	88.0	79.1
L-14	12	88.1	93.4	50	100.6	82.4	62	98.2	84.5	NA	NA
L-15	8	100.8	104.6	45	107.2	89.5	53	106.2	91.8	111.1	94.7

[a]Data obtained from both the methods agree well (within 0 to 5‰).

extracted from silver oxide then provide information about the intramolecular distribution of two (^{17}O and ^{18}O) heavy oxygen isotopes.

[9] For clarity, we organize the paper as follows. The details of the experiment are given in section 2. The isotopic composition of the reacting ozone, leftover oxygen and the oxygen extracted from silver oxide along with the information of r^{50} from the *Janssen* [2005] compilation were used to calculate the fractionation associated with ozone silver reaction. The procedure for calculating the value of fractionation and the intramolecular distribution of ^{17}O in ozone is described in section 3.1 and 3.2. In this connection an experiment designed to investigate the effect of catalysis on the isotopic composition of silver oxide is described in Appendix A. Appendix B describes in detail the calculation of abundances and related delta values of asymmetric and symmetric species of the two heavy ozone isotopologues using the known rate constants so that a comparison can be made with the results obtained here. Appendix C gives the error analysis of the experimental data. The present results are compared with the earlier results in section 3.3. Section 3.4 provides the application of the present study and the conclusions are presented in section 4.

2. Experimental Details

[10] The experiments were carried out in two places: the Laboratoire de Glaciologie et Géophysique de l'Environnement (LGGE), Grenoble, France, and the Physical Research Laboratory (PRL), Ahmedabad, India. At PRL, ozone was produced by two methods: (1) Tesla discharge of oxygen kept in a chamber (volume ~200 cm^3) at various pressures (a total of 27 samples) and (2) irradiation of oxygen (in a 5 L spherical chamber fitted with a MgF_2 side window, 2 mm thick and 2.5 cm diameter, at different pressures) with UV produced by a Hg resonance lamp (184.9 nm and 253.6 nm) driven by a microwave generator (in 17 cases). This provided an opportunity to compare the internal distribution of ozone produced by two different processes. At LGGE, ozone was produced only by Tesla discharge of oxygen (15 samples). In ozone production by Tesla discharge, both temperature of the chamber (−196°C to 80°C) and O_2 pressure were varied (from 15 to 50 torr) to get variable enrichments in the product ozone. However, the temperature of the "reaction zone" during Tesla discharge could not be defined because of large temperature gradient in the reaction chamber. In case of ozone made by UV dissociation only the O_2 pressure was varied (at room temperature from 30 to 1075 torr). The amount of ozone produced was always kept small relative to the oxygen reservoir (within about 10%). The product ozone was cryogenically separated from the leftover oxygen and was transferred to a small cold finger connected via a stopcock to a chamber containing precleaned silver foil. The silver was in the form of thin ribbon cut into several strands weighing approximately few mgs and cleaned by heating (>600°C) in vacuum ($<10^{-3}$ Torr). After complete transfer of ozone, the cold finger was isolated from the main line and ozone was brought in gaseous phase. The stopcock to the silver chamber was then opened quickly. Ozone instantaneously reacts with silver making a layer of grayish-blackish silver oxide. However, there is a parallel reaction whereby the major part of ozone gets decomposed almost simultaneously at the silver oxide surface by catalysis [*Waterhouse et al.*, 2001, 2002]. After a few minutes, the introduced ozone is completely decomposed by the combined process of reaction and catalysis. The oxygen produced in the chamber was collected in sample bottles containing molecular sieve (pellet 13 X) for amount and isotope measurements. Subsequently, the silver chamber was isolated from the main line and silver oxide (Ag_2O) was heated to ~500°C for 5–7 min using an external heater which releases the silver bound oxygen totally; this was collected in a molecular sieve kept at LN_2 for isotope analysis. The amount of initial ozone is obtained by adding the two components, namely, the oxygen left over after the reaction and the oxygen from silver oxide decomposition; the isotopic composition of starting ozone is determined by isotope mass balance from these two components (Table 1). In some cases, the mass balance estimate was crosschecked by taking an aliquot of

Table 2. Oxygen Isotopic Composition of Starting Ozone and Silver-Bound Oxygen[a]

	Ozone[b]			Ag_2O Oxygen				For ^{18}O in Ozone			For ^{17}O in Ozone			Error[d]	
Sample	Amount, μmol	$\delta_b^{18}O$	$\delta_b^{17}O$	Amount, μmol	$\delta^{18}O$	$\delta^{17}O$	Fractionation: $\alpha(^{18}O)$[c]	$\delta_a^{18}O$	$\delta_s^{18}O$	r^{50}	$\delta_a^{17}O$	$\delta_s^{17}O$	r^{49}	r^{50}	r^{49}
							PRL Data								
P-1	52	13.7	16.6	10	−1.4	22.4	0.9975	1.1	38.9	1.927	23.7	2.3	2.043	0.08	0.06
P-2	136	18.3	21.7	10	4.6	26.4	0.9974	7.2	40.5	1.936	27.7	9.6	2.036	0.08	0.06
P-3	122	22.0	23.9	13	13.9	35.8	1.0018	12.1	41.9	1.943	34.9	2.0	2.066	0.07	0.05
P-4	48	33.6	30.4	8	28.4	43.3	1.0010	27.4	46.2	1.964	42.8	5.7	2.074	0.07	0.05
P-5	25	34.5	35.1	9	13.6	34.5	0.9855	28.5	46.6	1.965	42.1	21.1	2.041	0.07	0.05
P-6	91	40.8	37.8	12	31.8	49.3	0.9953	36.7	49.1	1.976	51.8	9.7	2.083	0.07	0.05
P-7[e]	9	43.1	40.5	3	39.3	50.3	0.9997	39.6	50.0	1.980	50.5	20.5	2.059	0.07	0.05
P-8	57	44.4	41.0	10	38.5	54.7	0.9972	41.4	50.3	1.983	56.2	10.6	2.090	0.07	0.05
P-9	60	46.9	44.1	10	43.2	59.3	0.9987	44.6	51.7	1.986	60.0	12.2	2.094	0.06	0.05
P-10	71	47.2	41.8	9	45.5	59.1	1.0006	44.9	51.7	1.987	58.8	7.9	2.101	0.06	0.05
P-11	47	49.3	45.1	10	31.2	49.9	0.9842	47.8	52.5	1.991	58.3	18.6	2.078	0.06	0.05
P-12	17	51.1	43.3	3	25.3	40.9	0.9765	50.0	53.4	1.994	53.4	23.1	2.059	0.06	0.05
P-13	76	51.3	43.4	9	31.6	43.5	0.9823	50.2	53.5	1.994	52.9	24.5	2.055	0.06	0.05
P-14	30	51.9	47.6	4	43.9	56.9	0.9931	51.2	53.5	1.995	60.6	21.5	2.076	0.06	0.05
P-15[e]	38	54.7	51.3	7	44.8	55.2	0.9907	54.6	54.9	1.999	60.1	33.7	2.051	0.06	0.05
P-16	72	56.1	48.6	5	35.2	51.7	0.9799	56.4	55.3	2.002	62.4	20.8	2.082	0.06	0.05
P-17	36	59.0	53.0	5	46.0	58.1	0.9867	60.1	56.7	2.006	65.2	28.7	2.071	0.06	0.05
P-18	40	62.6	50.8	7	46.1	54.9	0.9825	64.7	58.2	2.012	64.3	23.9	2.079	0.06	0.05
P-19	76	67.4	63.7	11	71.2	83.1	1.0003	70.9	60.3	2.020	82.9	25.2	2.113	0.06	0.05
P-20	51	68.7	64.5	9	68.3	81.7	0.9960	72.6	61.0	2.022	83.9	25.7	2.113	0.05	0.05
P-21	96	69.1	63.9	12	71.5	83.3	0.9985	73.1	61.2	2.022	84.1	23.4	2.119	0.05	0.05
P-22	87	71.3	66.4	11	77.1	87.3	1.0012	75.8	62.1	2.026	86.6	26.0	2.118	0.05	0.05
P-23[e]	136	72.5	71.0	13	71.8	81.4	0.9947	77.5	62.5	2.028	84.3	44.5	2.076	0.05	0.04
P-24	46	77.3	70.3	8	76.3	87.4	0.9933	83.6	64.8	2.035	91.1	28.8	2.121	0.05	0.05
P-25	47	78.0	70.5	8	76.3	86.4	0.9924	84.5	65.0	2.037	90.6	30.3	2.117	0.05	0.05
P-26[e]	343	81.4	76.9	16	87.3	93.9	0.9987	88.7	66.7	2.041	94.6	41.5	2.102	0.05	0.04
P-27[e]	107	89.8	83.5	12	99.5	103.3	1.0001	99.4	70.7	2.054	103.2	44.0	2.113	0.04	0.04
P-28[e]	49	91.8	88.1	9	91.8	101.9	0.9908	101.9	71.5	2.057	107.0	50.4	2.108	0.04	0.04
P-29[e]	28	97.1	92.6	6	89.8	99.6	0.9830	108.6	74.1	2.064	109.1	59.6	2.093	0.04	0.04
P-30[e]	45	101.8	87.2	9	90.2	94.6	0.9782	114.5	76.5	2.071	106.7	48.2	2.112	0.04	0.04
P-31[e]	139	102.0	95.6	13	118.6	121.6	1.0035	114.7	76.6	2.071	119.9	47.0	2.139	0.04	0.04
P-32[e]	35	102.4	96.3	7.7	94.6	104.4	0.9815	115.2	76.8	2.071	114.8	59.3	2.105	0.04	0.04
P-33[e]	76	104.3	95.9	10	100.5	106.6	0.9847	117.6	77.7	2.074	115.2	57.4	2.109	0.04	0.04
P-34[e]	70	104.7	98.2	10	100.7	108.8	0.9844	118.1	78.0	2.075	117.6	59.5	2.110	0.04	0.04
P-35[e]	66	111.6	104.3	9	120.8	126.9	0.9948	126.7	81.3	2.084	129.8	53.3	2.145	0.03	0.04
P-36[e]	72	112.8	102.0	15	108.8	115.4	0.9828	128.2	82.1	2.085	125.1	55.7	2.132	0.03	0.04
P-37[e]	26	115.6	106.3	5	113.9	122.7	0.9843	131.7	83.5	2.089	131.6	55.7	2.144	0.03	0.04
P-38[f]	130	15.5	16.0	11	12.5	29.6	1.0089	3.6	39.5	1.931	25.0	−1.9	2.054	0.08	0.06
P-39[f]	12	26.3	25.3	3	−7.4	12.1	0.9754	17.7	43.5	1.951	24.8	26.2	1.997	0.08	0.05
P-40[f]	19	58.1	47.4	6	32.5	48.5	0.9750	59.0	56.3	2.005	61.9	18.5	2.085	0.06	0.05
P-41[f]	37	61.7	56.1	12	38.0	53.9	0.9759	63.6	57.9	2.011	66.8	34.5	2.062	0.06	0.05
P-42[f]	10	78.0	72.0	3	52.9	64.9	0.9709	84.5	65.2	2.036	80.8	54.6	2.050	0.05	0.04
P-43[f]	29	100.4	95.4	6	80.6	94.6	0.9712	112.7	75.8	2.069	110.7	64.7	2.086	0.04	0.04
P-44[f]	27	104.7	95.9	6	86.8	94.6	0.9720	118.1	77.9	2.074	110.2	67.3	2.080	0.04	0.04
							LGGE Data								
L-1	84	10.7	11.7	11	−1.4	17.4	1.0014	−2.8	37.7	1.922	16.7	1.6	2.030	0.08	0.06
L-2	58	20.7	21.7	8	5.0	25.8	0.9948	10.3	41.5	1.940	28.5	8.1	2.041	0.07	0.06
L-3	125	28.1	29.0	5	19.4	36.6	0.9995	20.0	44.3	1.953	36.9	13.3	2.046	0.07	0.05
L-4	99	39.4	40.4	10	26.0	45.5	0.9915	34.8	48.6	1.974	50.0	21.2	2.056	0.07	0.05
L-5	39	45.9	45.4	4	35.4	52.1	0.9926	43.2	51.3	1.985	56.0	24.2	2.062	0.07	0.05
L-6	84	52.3	51.6	10	42.1	58.2	0.9911	51.5	53.9	1.995	62.9	29.0	2.066	0.06	0.05
L-7	27	53.1	51.3	5	38.7	56.1	0.9868	52.9	54.3	1.997	63.1	27.5	2.069	0.06	0.05
L-8	119	60.7	57.1	3	58.2	66.3	0.9961	62.4	57.3	2.010	68.4	34.4	2.066	0.06	0.05
L-9	98	64.4	60.4	9	56.7	70.4	0.9902	67.1	58.9	2.016	75.7	29.6	2.090	0.06	0.05
L-10	126	76.4	70.4	9	72.6	82.2	0.9909	82.4	64.3	2.034	87.2	37.0	2.097	0.05	0.05
L-11	110	83.9	75.4	12	76.5	85.9	0.9859	91.9	67.9	2.045	93.6	39.1	2.105	0.05	0.04
L-12	84	84.1	76.6	6	81.0	88.5	0.9900	92.0	68.3	2.044	93.9	41.8	2.100	0.05	0.04
L-13	47	86.4	76.8	3	88.0	88.2	0.9936	95.0	69.0	2.049	91.7	47.0	2.085	0.05	0.04
L-14	62	98.2	84.5	12	88.1	93.4	0.9840	109.9	74.8	2.065	104.2	45.1	2.113	0.04	0.04
L-15	52	106.2	91.8	8	100.8	104.6	0.9829	120.0	78.6	2.077	114.1	47.2	2.128	0.03	0.04
							Zero Enriched Data								
1	63	−9.5	−5.5	10	−55.7	−26.8	0.9916[g]	−47.2	65.9	1.788	−22.4	28.3	1.901	NA	NA
2	38	−8.9	−4.4	9	−57.6	−28.8		−49.1	71.6	1.755	−24.4	35.6	1.884		
3	150	−8.8	−4.9	16	−47.5	−19.3		−38.9	51.3	1.828	−14.9	15.3	1.941		
4	135	−8.2	−4.2	12	−46.7	−19.4		−38.1	51.6	1.829	−15.0	17.4	1.936		
5	91	−7.5	−3.7	13	−48.9	−22.2		−40.4	58.2	1.814	−17.8	24.5	1.917		
6	124	−6.3	−3.5	33	−40.0	−13.2		−31.4	43.7	1.856	−8.8	6.9	1.969		
7	75	−5.4	−3.3	16	−40.8	−14.4		−32.2	48.3	1.846	−10.0	10.2	1.960		

Table 2. (continued)

	Ozone[b]			Ag_2O Oxygen				For ^{18}O in Ozone			For ^{17}O in Ozone			Error[d]	
Sample	Amount, μmol	$\delta_b^{18}O$	$\delta_b^{17}O$	Amount, μmol	$\delta^{18}O$	$\delta^{17}O$	Fractionation: $\alpha(^{18}O)$[c]	$\delta_a^{18}O$	$\delta_s^{18}O$	r^{50}	$\delta_a^{17}O$	$\delta_s^{17}O$	r^{49}	r^{50}	r^{49}
8	201	−4.6	−2.1	14	−36.0	−11.2		−27.3	40.7	1.869	−6.8	7.2	1.972		
9	134	−3.7	−2.1	16	−33.7	−9.0		−25.0	39.0	1.877	−4.5	2.9	1.985		

[a]For both $^{17}O^{16}O_2$ and $^{18}O^{16}O_2$, enrichment in terminal and central positions increases with the increase in bulk ozone enrichment. The values of r^{49} vary from 2.030 to 2.145 which are higher than the r^{50} values (from 1.922 to 2.089).
[b]Starting ozone amount and isotopic composition were calculated by mass balance.
[c]The value of $\alpha(^{18}O)$ was calculated using the measured value of $\delta^{18}O(Ag_2O)$ and $\delta_a^{18}O$.
[d]Total error calculated in r^{50} and r^{49} (see Appendix C).
[e]In these cases ozone was made by UV dissociation of O_2 (others were made by Tesla discharge).
[f]These data points fall beyond 1.5 σ (−8.4 ± 15‰) and therefore rejected (see Figure 4).
[g]Average value of the fractionation (α = 0.9916 or ε_t = −8.4‰) calculated for enriched cases.

the initial ozone (Table 1). However, we prefer to use the mass balance estimate for total initial ozone since taking proper aliquot of ozone which is isotopically as well as quantitatively representative turned out to be time consuming and difficult.

[11] A relevant point of interest is whether catalytic decomposition of ozone by silver oxide formed at the first phase of the process alters the isotopic composition of silver oxide itself. This issue was addressed by a few control experiments and is described in detail in Appendix A. The control experiments show that it is possible to alter the isotopic composition of Ag_2O if the ozone undergoing catalysis is itself significantly different in composition. Since the reaction and catalysis took place very fast in an uncontrolled manner the final isotopic composition of Ag_2O had large variability due to variable contribution from the above two sources of fractionation.

[12] Beside the case of isotopically enriched ozone it is also of interest to determine the internal distribution of heavy oxygen isotopes in an ozone sample which is not enriched (in the sense described above) relative to the oxygen gas from which it is made. For this purpose, ozone was made by converting nearly 100% of the starting O_2 by Tesla discharge (designated as zero-enriched ozone). In these cases, the amount of starting O_2 was kept low (the pressure in the chamber being between 3 to 15 Torr).

[13] Molecular oxygen isotopic measurements were done with a Finnigan MAT 253 at LGGE with typical errors of 0.05‰ on both $\delta^{18}O$ and $\delta^{17}O$ and with a VG 903 at PRL with typical errors of 0.05‰ and 2‰ in $\delta^{18}O$ and $\delta^{17}O$ respectively. The larger error in $\delta^{17}O$ in the old VG machine is due to its lower sensitivity and a low signal-to-noise ratio. Amount of oxygen was measured using MKS Baratron in both places. The isotopic composition of the tank O_2 at PRL ($\delta^{18}O$, $\delta^{17}O$ relative to VSMOW) was (24.6, 12.5) and that at LGGE was (12.1, 6.0).

3. Results and Discussion

[14] The oxygen isotopic composition of ozone and silver-bound oxygen (Ag_2O) (expressed relative to the tank oxygen) for PRL and LGGE experiments are given in Table 2. $\delta^{17}O$ values plotted against $\delta^{18}O$ values for Ag_2O and for ozone (Figure 1) define two parallel lines showing the effect of associated fractionation. Figure 1 suggests that even though the δ values are different, the characteristics of the ozone isotopic distribution are preserved in its reaction with silver. The results are also displayed in Figure 2 where $\delta(Ag_2O)$ values are plotted against $\delta_b(O_3)$ values for each of the two heavy isotopes. It is seen that both $\delta^{18}O$ and $\delta^{17}O$ values of Ag_2O increase linearly with increase in ozone δ values in nearly parallel fashion; the cross plots define two best fit lines with slopes 1.16 ± 0.04 (^{18}O) and 1.12 ± 0.03 (^{17}O). It is intriguing to note on a first sight that the $\delta^{18}O$ values of Ag_2O are mostly less than those of ozone, i.e., $\delta^{18}O$ (Ag_2O) < $\delta_b^{18}O$ (O_3) whereas in case of $\delta^{17}O$ it is mostly the other way around, i.e., $\delta^{17}O$ (Ag_2O) > $\delta_b^{17}O$ (O_3). In PRL experiments, the $\delta^{18}O$ and $\delta^{17}O$ values of Ag_2O vary from −1.4 to 120.8 and 22.4 to 126.9 respectively corresponding to a variation of 13.7 to 115.6 and 16.6 to 106.3 in the δ values of ozone. In case of LGGE experiments, variations of $\delta^{18}O$ and $\delta^{17}O$ values of Ag_2O from −1.4 to 100.8 and from 17.4 to 104.6 correspond to variations of 10.7 to 106.2 and 11.7 to 91.8 respectively in the δ values of ozone.

[15] The oxygen isotopic compositions of zero-enriched ozone are also given in Table 2 and shown in Figure 1. As before, the ozone isotopic composition was determined by mass balance. It is noted that in this case the collected ozone is slightly *depleted* in heavy oxygen isotopes relative to the cylinder oxygen in a nearly mass-dependent fashion. The $\delta^{18}O$ and $\delta^{17}O$ values of ozone vary from −9.5 to −3.7 and −5.5 to −2.1 corresponding to pressure variation in initial oxygen from 3 to 15 Torr. Ideally, these δ values should be zero if one can completely convert the molecular oxygen to ozone. However, during these cases the speed of ozone formation reduces very much when the residual pressure reaches about 0.2 Torr in the Tesla chamber and one has to stop the discharge to go ahead with the rest of the experiment. This means that there is about 5% unconverted oxygen left in the chamber. It is known from an early experiment of *Bains-Sahota and Thiemens* [1987] who used microwave discharge in a flow system that at low pressures (less than 25 Torr) the isotope selectivity in ozone reverses and there is depletion of heavy oxygen isotopes which follows a $\delta^{17}O$-$\delta^{18}O$ slope of ∼0.7. This is because at very low pressures, preferential wall recombination of heavy oxygen atoms interferes with the process. We also believe that in our case because of partial contribution from such heterogeneous processes, the total accumulated ozone shows slightly negative δ values in going from a pressure of 3–15 Torr down to ∼0.2 Torr. There is a radical change

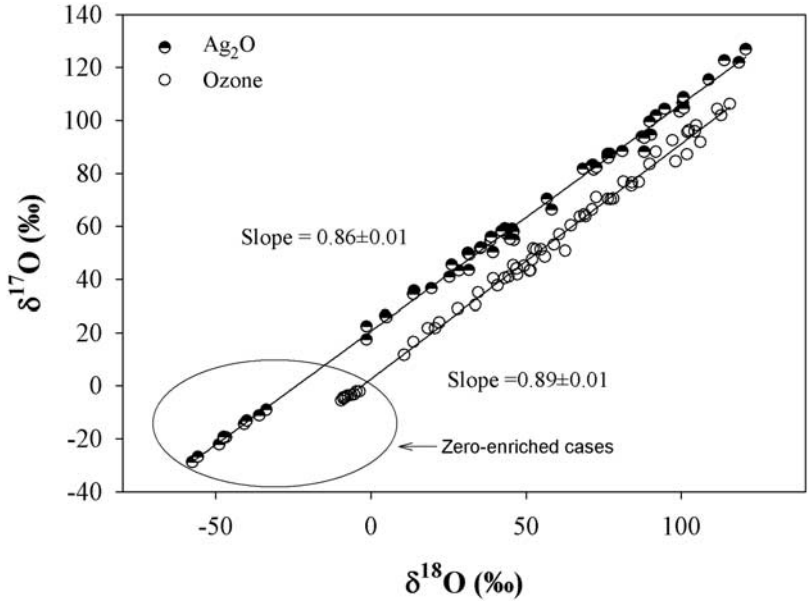

Figure 1. Cross plot of $\delta^{18}O$ and $\delta^{17}O$ values (expressed in ‰ relative to the initial oxygen reservoir) of Ag_2O and starting ozone for both LGGE and PRL experiments. The $\delta^{18}O$ and $\delta^{17}O$ values of Ag_2O and O_3 fall on lines with slope 0.86 ± 0.01 and 0.89 ± 0.01, respectively, showing that the characteristics of ozone are preserved in silver oxide.

in the δ values of Ag_2O in these cases. They are found to be highly depleted in both the heavy isotopes compared to the enriched ozone cases. The values of $\delta^{18}O$ and $\delta^{17}O$ of Ag_2O vary from −55.7 to −33.7 and −26.8 to −9.0 corresponding to the variation in ozone mentioned above. As we shall see, this contrast is directly related to a totally different internal distribution of heavy isotopes in zero-enriched ozone.

3.1. Fractionation During Ozone Silver Reaction

[16] As mentioned before, during the reaction of ozone with silver, oxygen atoms in the ozone reservoir get

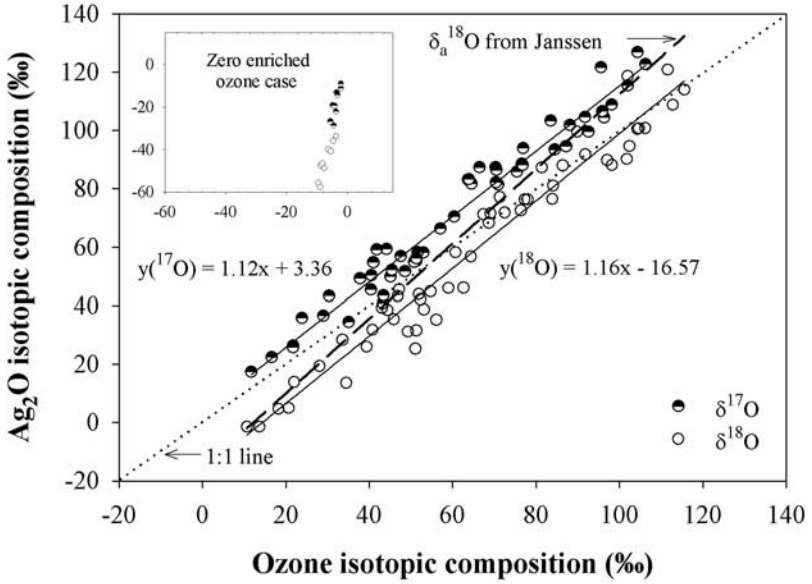

Figure 2. Correlation plot of $\delta(Ag_2O)$ and $\delta(O_3)$ showing that δ values of silver-bound oxygen increase with increase in ozone δ values in a linear fashion for both ^{17}O and ^{18}O. The $\delta^{18}O$ values of Ag_2O are less than those of reacting O_3 because of chemical fractionation. In contrast, the $\delta^{17}O$ values of Ag_2O are higher than those of O_3 because of fractionation and large position-dependent enrichment. The enrichment in terminal position (as calculated from the work by *Janssen* [2005]) is plotted to show the effect of fractionation. Samples with negligible enrichment (zero-enriched cases) have very different δ values of Ag_2O as shown in inset.

distributed in two phases: a solid phase where oxygen atoms (about 10 to 15% of total) are chemically bound as silver oxide and a gaseous phase comprising oxygen generated in two processes: (1) oxygen molecules produced by reaction of ozone with silver ($O_3 + 2Ag \rightarrow Ag_2O + O_2$) and (2) oxygen molecules produced by secondary catalytic reaction of ozone with freshly formed silver oxide ($2O_3 + Ag_2O \rightarrow Ag_2O + 3O_2$).

[17] It is clear from Figure 2 that though the δ values of silver oxide are linearly related to the ozone δ values they are different from those of ozone; while the $\delta^{17}O$ is slightly enriched, the $\delta^{18}O$ is slightly depleted suggesting a type of mass-dependent fractionation. The total fractionation (ε_{tot} of silver oxide relative to ozone) possibly comprises two parts: (1) a fractionation due to kinetic effect (ε_k) associated with the chemical reaction initiated by the ozone gas which diffuses into the silver chamber and reacts rapidly with the silver foil and (2) a fractionation due to catalytic decomposition (ε_{cat}) of ozone by freshly formed silver oxide. Part of the kinetic fractionation arises because of different bond strengths of various ozone isotopologues. The formation of silver oxide involves breakage of one O-O bond in ozone followed by formation of one Ag-O-Ag bond. It is well known that ^{16}O-^{16}O bond breaks more easily compared to ^{16}O-^{18}O bond because of its higher zero point energy. For example, if only the terminal atom extraction is involved the values of asymmetric stretch frequency of ozone molecules $^{16}O^{16}O^{18}O$ (1090 cm^{-1}) and $^{16}O^{16}O^{16}O$ (1103 cm^{-1}) lead one to expect a faster dissociation rate of the second molecule by about 12‰ [(1103/1090)−1 = 11.9‰]. However, this is only a part of the whole process; the production of silver oxide most likely proceeds through two steps: formation of a transient complex involving ozone and silver atoms and the breakup of this complex where formation of $Ag_2^{18}O$ would be preferred over $Ag_2^{16}O$ because of zero point energy effect. The net result of these three effects (diffusion, complex formation and complex break down) determines whether the silver-bound oxygen is depleted or enriched in heavy isotopes. On the basis of theoretical reaction rate studies of isotopic molecules [*Bigeleisen and Wolfsberg*, 1958], one normally expects lighter species to have a faster reaction rate leading to isotopic depletion in silver oxide. Such expectation is supported by an early study of *Dole et al.* [1954] who showed that lighter oxygen isotopes are chemisorbed preferentially on metal surfaces.

[18] The catalytic fractionation arises because of catalytic dissociation of ozone by newly formed silver oxide. In the present experimental configuration ozone interaction with silver can be visualized as a process in which a continuous stream of ozone molecules impinges on silver surface and reacts quickly covering the silver foil with freshly formed Ag_2O. The subsequent incidence of ozone molecules occurs on this preformed Ag_2O surface whereby only catalytic dissociation could occur. Since the later batch of ozone molecules are expected to be heavier, it is likely that this heavier ozone exchanges partly with the lighter oxygen of the preformed silver oxide phase. Consequently, the catalytic fractionation probably acts toward increasing the δ value of Ag_2O. As in kinetic fractionation, the net effect of catalytic fractionation is not constant and depends on various parameters governing the reaction and catalysis, like condition of the metal surface, ozone amount and its isotopic composition. A set of control experiments carried out to determine this effect showed that if the difference between the initial ozone and the next batch of ozone is large (>7‰) the change could be appreciable (see Appendix A). Thus, though the net fractionation is expected to be determined by the balance between these fractionations and can vary depending on the relative contribution of each of them, on an average, we expect it to lower the silver oxide δ value relative to that of ozone.

[19] In addition to fractionation, we also have to consider whether the oxygen atom is extracted from the central position or the terminal position of ozone in forming the silver oxide. As mentioned before, it is highly probable that the reaction occurs mostly with the terminal atoms [*Babikov et al.*, 2003]. In addition, the hypothesis of terminal atom reaction helps to explain the intriguing difference between $\delta^{17}O$ and $\delta^{18}O$ of Ag_2O, i.e., why $\delta^{17}O$ of Ag_2O is mostly higher than that of bulk ozone whereas $\delta^{18}O$ is lower. As discussed, a lower $\delta^{18}O$ (Ag_2O) is easily explained by a net depletion due to fractionation. However, in case of ^{17}O the situation is different. Even though the $\delta_b^{17}O$ value of bulk ozone is nearly equal to its $\delta_b^{18}O$ value, the fractionation in ^{17}O (being mass-dependent) is only half that of ^{18}O. Now, if the $\delta^{17}O$ value of terminal position is higher than that of bulk ozone by an amount more than the ^{17}O fractionation we may get $\delta^{17}O$ (Ag_2O) > $\delta_b^{17}O(O_3)$ even when $\delta^{18}O$ (Ag_2O) < $\delta_b^{18}O$ (O_3) (Figure 3). The contrasting pattern between $\delta^{17}O$ and $\delta^{18}O$, therefore, seems consistent with our assumption that terminal atoms of ozone are the ones to react with silver (albeit with a fractionation factor less than one).

3.2. Calculation of $\delta_a^{17}O$, $\delta_s^{17}O$, and r^{49}

[20] The $\delta^{17}O$ values of the oxygen extracted from silver oxide can be used to calculate the $\delta^{17}O$ values of the terminal position of ozone (i.e., $\delta_a^{17}O$) if one can correct for the associated fractionation for ^{17}O. Since the $\delta^{18}O$ values for both silver oxide and ozone are also available simultaneously they can be used to obtain the net fractionation for ^{18}O in each sample and then using the mass dependence law for chemical fractionation one can derive the value for ^{17}O fractionation in the corresponding sample. Once we obtain the $\delta_a^{17}O$ value, the $\delta_s^{17}O$ can be calculated by using the intramolecular isotope balance law and the $\delta_a^{17}O$ and the $\delta_s^{17}O$ values in turn determine the r^{49} value for each sample. The detailed steps are described below. Since the isotope ratio is always expressed relative to the starting oxygen reservoir the measured δ values themselves represent the enrichment.

[21] Our method depends critically on the analytical results of *Janssen* [2005] who carefully evaluated all the earlier FTIRS and TDLAS data and tabulated the values of r^{50} for a set of ozone enrichment values ranging from 6‰ to 156‰. On the basis of this compilation we get the following equation relating the ^{18}O enrichment in asymmetric species ($\delta_a^{18}O$) with bulk ozone enrichment ($\delta_b^{18}O$) (in ‰) as:

$$\delta_a^{18}O = -17.04 + 1.33 \times \left(\delta_b^{18}O\right) - 3.93 \times 10^{-4} \times \left(\delta_b^{18}O\right)^2 \quad (3)$$

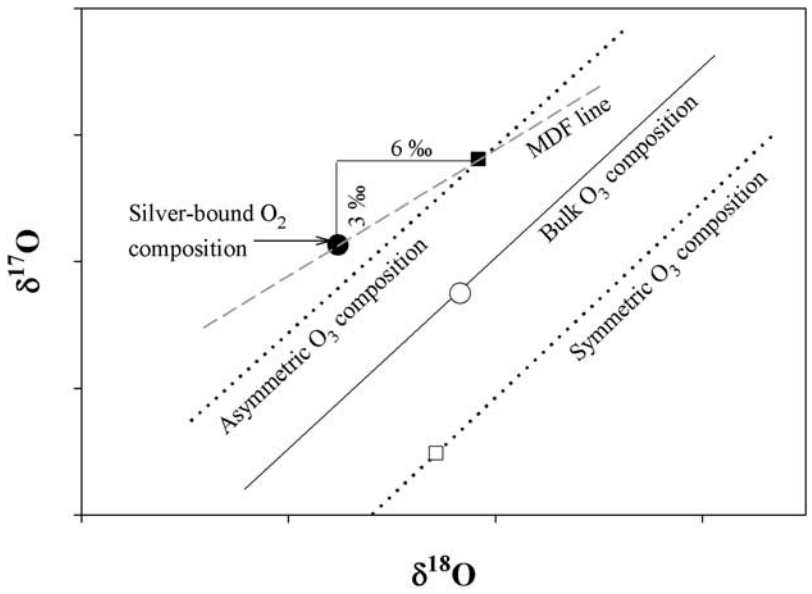

Figure 3. A schematic diagram showing relationship among the enrichments corresponding to the bulk, symmetric and asymmetric ozone. It is clear that for small fractionation values (~6‰ in ^{18}O), $\delta^{17}O$ (Ag_2O) > $\delta_b{}^{17}O$ (O_3) but $\delta^{18}O$ (Ag_2O) < $\delta_b{}^{18}O$ (O_3). It is also seen that only the terminal atoms (asymmetric ozone) are involved; otherwise it would be impossible to produce $\delta^{17}O$ (Ag_2O) > $\delta_b{}^{17}O$ (O_3). MDF line indicates mass-dependent fractionation line.

We assume that the above relation is valid in our case and apply it to calculate the expected enrichment in asymmetric species, i.e., $\delta_a^{18}O$ corresponding to each ozone enrichment value $\delta_b^{18}O$ obtained in the present experiment (see Table 2).

[22] The initial ozone isotopic composition $\delta_b^{18}O$ indicating "total enrichment" in bulk ozone can be expressed in terms of asymmetric $\delta_a^{18}O$ and symmetric $\delta_s^{18}O$ enrichment as:

$$\delta_b^{18}O = (\delta_s^{18}O + 2\delta_a^{18}O)/3 \quad (4)$$

$\delta_s^{18}O$ and $\delta_a^{18}O$ are multiplied by 1/3 and 2/3 because the statistical weight is two times higher for the asymmetric type compared to the symmetric type. The above relations implicitly assume that the internal distribution is strictly determined by the bulk enrichment value regardless of the process and pressure/temperature conditions of formation which can slightly change from one sample to another. We cannot rule out some variations in the internal distribution for a given enrichment level but expect them to be small on the basis of earlier works.

[23] In case of silver ozone interaction, assuming reaction by the terminal atoms only, the observed isotopic composition of silver oxide $\delta^{18}O(Ag_2O)$ should be determined only by $\delta_a^{18}O$ except for a correction due to chemical fractionation. In terms of isotope ratio $^{18}O/^{16}O = R^{18}$, one can, therefore, write

$$R_a^{18}(O_3) = R^{18}(Ag_2O)/\alpha^{18} \quad (5)$$

[24] The fractionation factor α^{18} was calculated in each case by using $\delta^{18}O(Ag_2O)$ and $\delta_a^{18}O$ obtained by equation (3). The combined LGGE (total 15) and PRL (total 44) data (Table 2) show that the fractionation factor α^{18} is not constant but varies from 1.0089 to 0.9709; that is, fractionation factor can be both less or more than one. When all samples are considered (a total of 59) a near normal distribution is seen in the frequency plot of $\varepsilon_{tot} = (\alpha^{18}-1) \times 1000$ (Figure 4) with mean of −10.0 and standard deviation of 10.0. This probably indicates that there is some randomness in the relative contribution of the fractionating processes and possibly the internal distribution for a given bulk enrichment is not absolutely constant but slightly variable. From the whole data set, six PRL samples having very low fractionation value (with ε_{tot} −24 to −30‰) and one having highly positive value (8.9‰) were considered unreliable and rejected. The samples with ε_{tot} values within 1.5 σ (σ = standard deviation, i.e., data lying within +3.8 to −23.8‰) of the modified mean (−8.4‰ corresponding to a total of 37 (PRL) +15 (LGGE) = 52 samples) were only considered for further analysis. The accepted set of 52 samples has fractionation factor ranging from 1.0035 to 0.9765. The minimum value of ε_{tot} (−23‰) probably denotes the maximum extent of kinetic fractionation (ε_k) and the spread in the values from −23 to +3.5 could be due to additional contributions as discussed above.

[25] Given the fractionation factor for ^{18}O, the fractionation factor for ^{17}O (α^{17}) can be derived by assuming the fractionation to be mass-dependent, i.e., $\alpha^{17} = (\alpha^{18})^{0.515}$. Using the measured δ value of silver oxide $\delta^{17}O(Ag_2O)$ and the derived α^{17}, enrichment in asymmetric species $\delta_a^{17}O$ can be calculated in each case. Using this value and calculating $\delta_s^{17}O$ from equation (4), values of r^{49} for ^{17}O can then be obtained using the formula

$$r^{49} = 2 \times (1 + 10^{-3} \times \delta_a^{17}O)/(1 + 10^{-3} \times \delta_s^{17}O) \quad (6)$$

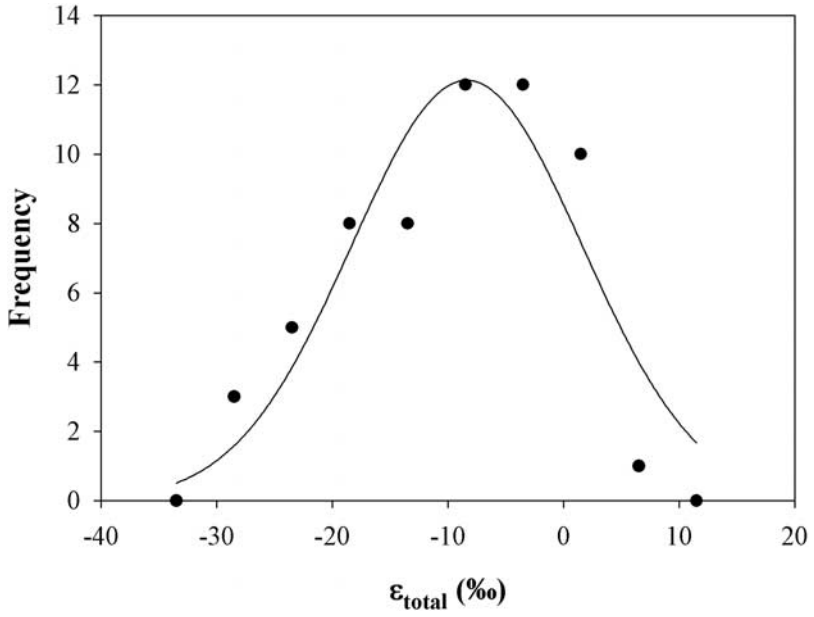

Figure 4. Frequency distribution of ε_{total} values (as defined in text) calculated for $^{18}O/^{16}O$. The spread of ε_{total} values is due to variable fractionation effects associated with the ozone silver reaction described in the text.

[26] The calculated r^{49} values are given in Table 2 and they vary from 2.030 to 2.145. In contrast, the r^{50} values vary from 1.922 to 2.089. r^{49} values are calculated in several steps and each step contributes some uncertainty leading to overall uncertainty in the calculated values. The procedure for estimating the overall uncertainty in r^{49} values is discussed in detail in Appendix C which shows that the total error values range from 0.04 to 0.06. The $\delta_a^{17}O$, $\delta_s^{17}O$ and r^{49} values (Table 2) show that in case of ^{17}O also, both terminal and central positions are enriched but with extra preference for terminal position at all enrichment levels. In case of ^{18}O, an increase in bulk enrichment in $^{18}O^{16}O_2$ from 13.7 to 115.6‰ corresponds to an increase in enrichment from 1.1 to 131.7‰ in asymmetric species and 38.9 to 83.5‰ in symmetric species. For ^{17}O, the bulk enrichment range of (16.6 to 106.3‰) corresponds to enrichment range of (23.7 to 131.6‰) and (2.3 to 55.7‰) in asymmetric and symmetric species respectively. The $\delta^{17}O$-$\delta^{18}O$ correlation plots (Figure 5) for bulk ozone, asymmetric type and symmetric type of ozone show different slopes and range of values for the three types.

[27] It is interesting to note that the intramolecular distributions for ^{18}O and ^{17}O are not the same. The mean difference between r^{49} and r^{50} is 0.075 ± 0.026 (Appendix C). The

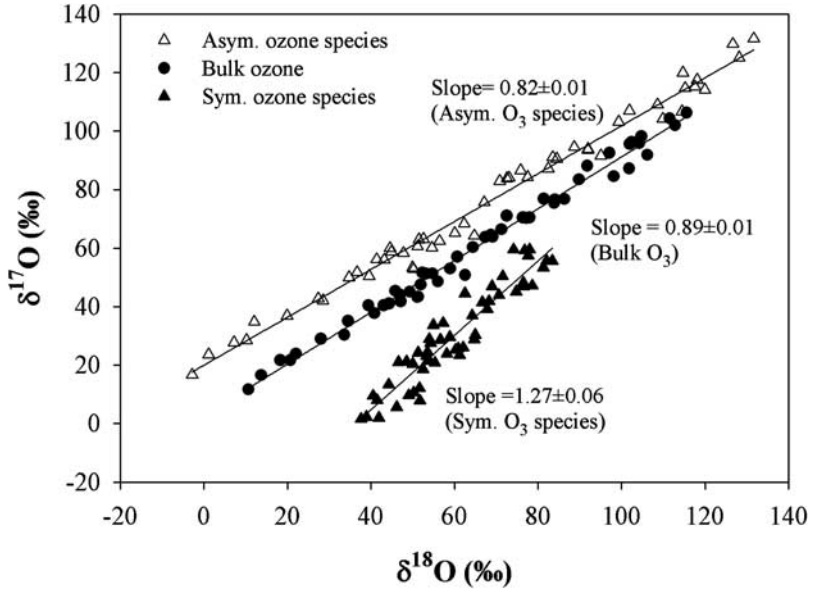

Figure 5. The $\delta^{17}O-\delta^{18}O$ correlation plot for bulk ozone, symmetric ozone, and asymmetric ozone showing different characteristics of the three species.

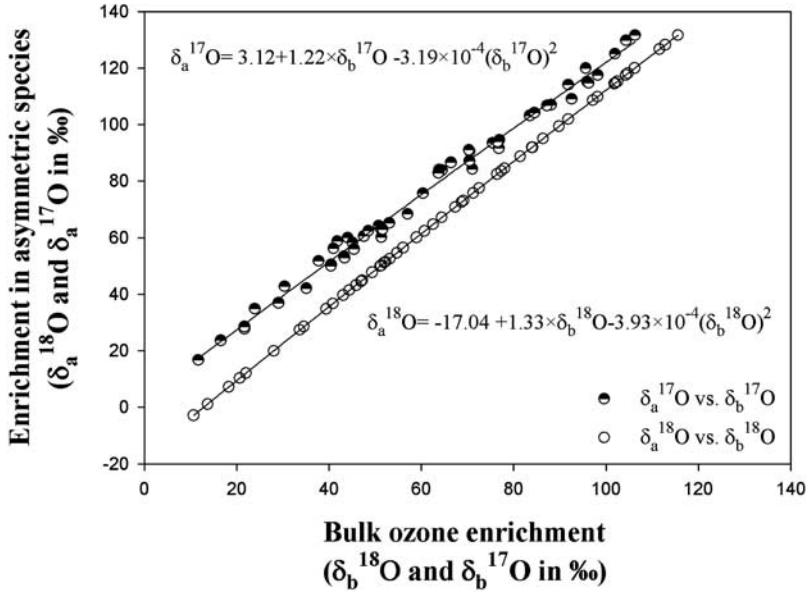

Figure 6. Enrichment in asymmetric species plotted against bulk enrichment for both PRL and LGGE data (see Table 1) showing different behavior of ^{18}O and ^{17}O species. At ozone enrichment values higher than ~50 ‰ the terminal position is enriched in both ^{18}O and ^{17}O compared to the bulk enrichment. The difference between the enrichments in two asymmetric species (i.e., ^{18}O and ^{17}O) decreases with increase in bulk enrichment.

difference between terminal and central position enrichments is more in case of $^{17}O^{16}O_2$ than in case of $^{18}O^{16}O_2$. This finding is consistent with an independent calculation of r^{50} and r^{49} using the values of relative rate coefficient of formation of asymmetric and symmetric species obtained from *Janssen et al.* [2001] which shows higher value of r^{49} relative to r^{50} (for a specific ozone enrichment level; see Appendix B). For both $^{18}O^{16}O_2$ and $^{17}O^{16}O_2$, the difference between the two enrichments is not constant but decreases with increase in the bulk ozone enrichment (compare the trends in Figures 6 and 7). We derive the following equation by fitting a best fit line relating the enrichment in ^{17}O of asymmetric species with that of bulk ozone (δ values in ‰):

$$\delta_a^{17}O = 3.12 + 1.22 \times (\delta_b^{17}O) - 3.19 \times 10^{-4} \times (\delta_b^{17}O)^2 \quad (7)$$

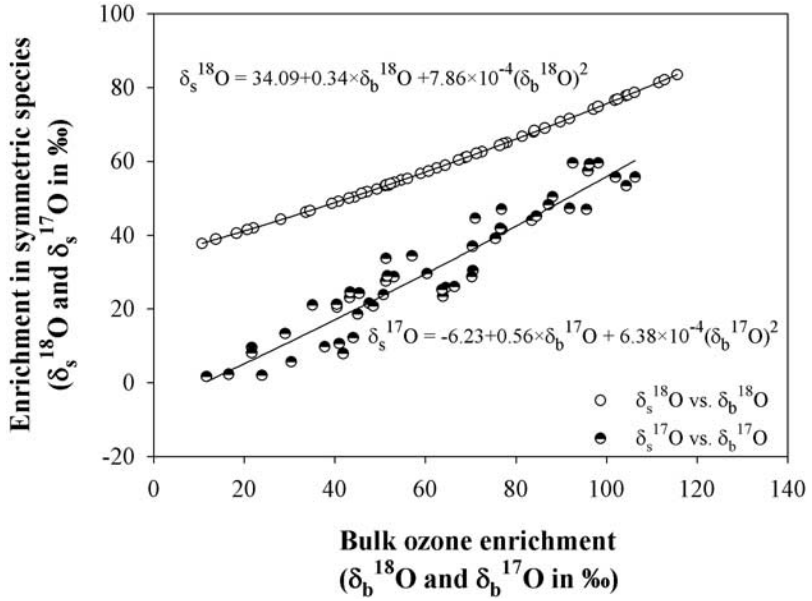

Figure 7. Enrichments in $^{18}O/^{16}O$ and $^{17}O/^{16}O$ at the central position of the ozone molecule plotted against bulk enrichment showing different behavior of ^{18}O and ^{17}O species. The difference between the enrichments in two symmetric species (i.e., ^{18}O and ^{17}O) decreases with increase in bulk enrichment.

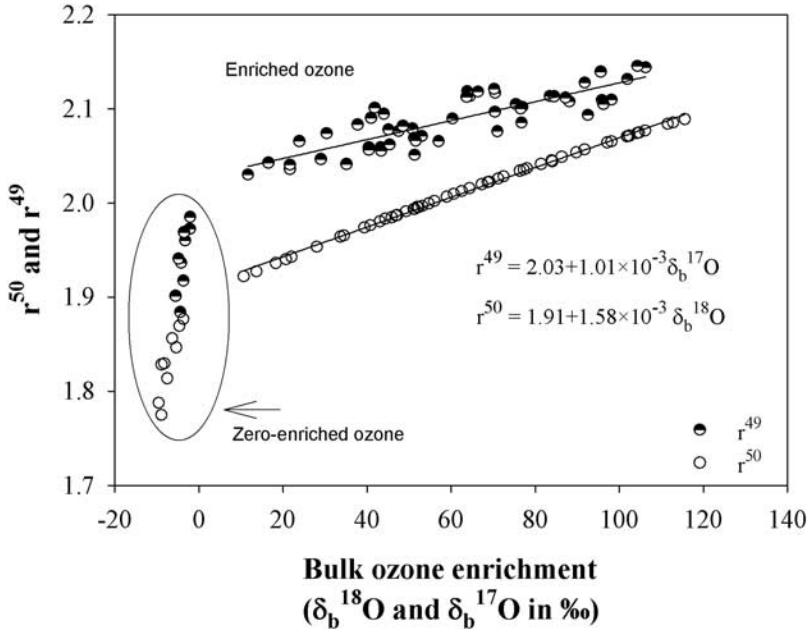

Figure 8. Ratio of asymmetric to symmetric species for $^{18}O^{16}O_2$ and $^{17}O^{16}O_2$ (as defined in terms of r values) plotted against the bulk ozone enrichment. The values of r^{49} are more than those of r^{50} indicating different internal distribution of two heavy isotopes in $^{18}O^{16}O_2$ and $^{17}O^{16}O_2$ isotopologues. The value of r^{49} varies from 2.04 to 2.15 corresponding to variation in bulk ozone enrichment from ~16 to ~106‰ (in $^{17}O/^{16}O$).

[28] PRL data show a variation of r^{49} from 2.030 to 2.145 (Table 2). In contrast to r^{50}, r^{49} value never goes below 2.00 for enriched ozone. The ratios r^{50} (using equation of *Janssen* [2005]) and r^{49} are plotted against the bulk enrichment values in ^{18}O and ^{17}O respectively in Figure 8. In each case, there is a systematic increase in the ratio with bulk enrichment suggesting a more rapid increase in enrichment of asymmetric species over that of symmetric one. It is satisfying to note that the extrapolated value of r^{49} for a bulk enrichment of 122.5‰ is 2.154 which is close to the value 2.160 calculated using estimates of relative rate coefficient of symmetric and asymmetric ozone formation channels for this particular enrichment (discussed in Appendix B). The agreement lends credence to the hypothesis of terminal atom reaction.

[29] It is possible to relax the assumption of terminal atom reaction and still do the analysis. As an academic exercise, we analyzed the data for two such cases by assuming that the terminal atoms react in 95% and 90% of the time, i.e., by taking the terminal atom reaction probability, defined as "x," to be 0.95 and 0.90 instead of 1.00. It is observed that the estimated values of r^{49} in these cases (x = 0.95 and 0.90) are higher than those of x = 1.00 case. The values of r^{49} change from the range 2.030 to 2.145 to the range 2.061 to 2.192 when x changes from 1.00 to 0.90 (see Figure 9).

[30] In case of zero-enriched ozone, the analysis is constrained since the value of fractionation factor cannot be calculated by the procedure mentioned above because equation (3) is valid only in cases where the ozone is enriched and made by converting a small fraction of the oxygen reservoir so that the isotopic composition of the reservoir remains essentially unchanged. However, to make an approximate comparison of r^{49} and r^{50} values in zero-enriched cases with that of enriched cases, the average value of the fractionation factor as derived for enriched cases, i.e., 0.9916 (corresponding to the mean ε_t value of −8.4‰) is assumed for ^{18}O. Under this assumption, the values of r^{50} and r^{49} are always less than two. The variation in r^{50} is from 1.755 to 1.877 whereas the variation in r^{49} is from 1.884 to 1.985. It is apparent that the assumption of a constant fractionation value by disregarding any possible variation results in a large spread of r values even though all points refer to zero-enriched ozone samples (Figure 8). It is interesting to note that for zero-enriched ozone the symmetric species is more enriched in ^{18}O and ^{17}O compared to the asymmetric species which is opposite to what is observed in case of enriched ozone samples. We may mention here that for zero-enriched ozone (made by near complete conversion of oxygen) r values less than two are quite expected. In a closed system, as the oxygen is quantitatively converted to ozone, several changes take place. The oxygen bath itself changes its isotopic composition and the pressure reduces to levels where O_3 starts to form with depleted heavy isotopes in nearly mass-dependent fractionation pattern [*Bains-Sahota and Thiemens*, 1987; *Heidenreich and Thiemens*, 1985]. Finally, when nearly 100% of oxygen is converted to ozone the net fractionation is, of course, very small but the distribution of a heavy isotope (^{17}O or ^{18}O) inside the molecule is expected to be determined solely by ZPE consideration. Since symmetric ozone has the heavy isotope located in more tightly bound position it will be preferentially abundant compared to the purely statistical distribution (i.e., r = 2.00). A simple consideration of ZPE of $^{16}O^{18}O^{16}O$ (2776 cm^{-1}) and $^{16}O^{16}O^{18}O$ (2840 cm^{-1}) yields a vibrational partition function ratio of 1.070 which

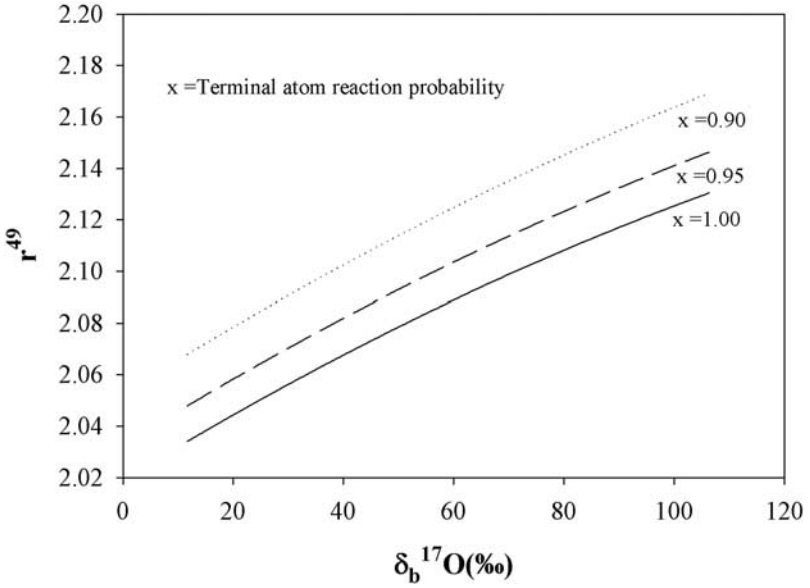

Figure 9. Values of r^{49} as function of the bulk ^{17}O enrichment for various values of terminal atom reaction probability x (x = 1, 0.95 and 0.90). The r^{49} values increase by 0.03 to 0.05 in going from x = 1 to x = 0.90.

suggests that the symmetric species will be more enriched by at least 70‰ which is close to the lower end of the values observed.

[31] Using the values of relative rate coefficients, the bulk enrichment as well as that in asymmetric and symmetric species for both ^{18}O and ^{17}O at 300 K were calculated (see Appendix B) which shows that r^{49} (2.160 ± 0.133) is indeed more than r^{50} (2.119 ± 0.102). The reason for the difference in the internal distributions of ^{17}O and ^{18}O can be inferred on the basis of the argument of *Janssen et al.* [2001] linking ΔZPE with the lifetime of the collision complex and the attainment of stability of a particular ozone isotopic configuration. If the pathway leading to the asymmetric type of ozone is linked with an exchange which has positive ΔZPE the complex has a larger lifetime which leads to a higher rate of stable ozone formation. This factor acts in favor of both ^{17}O and ^{18}O asymmetric species. However, the mass-dependent exchange favors ^{17}O relative to ^{18}O in the atomic oxygen pool which acts in favor of asymmetric ^{17}O species relative to asymmetric ^{18}O species. Together, the asymmetric to symmetric ratio in case of ^{17}O is slightly favored and we get $r^{49} > r^{50}$. As mentioned before, our method depends crucially on the validity of Janssen equation. The weakness of this approach lies in complete acceptance of Janssen prediction while the strength lies in deducing relative distribution of ^{17}O accurately as compared to ^{18}O. It is also to be noted that there is no significant variation in the internal distribution between ozone samples produced by Tesla discharge or by UV photolysis of oxygen.

3.3. Comparison With Earlier Work

[32] *Janssen and Tuzson* [2006] and *Tuzson and Janssen* [2006] have published recently two interesting papers dealing with techniques of TDLAS measurement of internal distribution of ^{18}O in ozone. *Tuzson* [2005] also tried to estimate the relative rate coefficient for both ^{18}O and ^{17}O species using the same technique. However, his result on symmetric ^{18}O species in particular does not agree with the earlier TDLAS study [*Janssen et al.*, 1999] and they state that "the origin of the higher enrichment found for $^{16}O^{18}O^{16}O$ in the earlier experiment remains yet unexplained" [*Janssen and Tuzson*, 2006]. Consequently, there is a big discrepancy (in ^{18}O species) between the enrichment values of asymmetric and symmetric species of ozone obtained by *Tuzson* [2005] and those given by *Janssen* [2005] compilation. We note that the enrichment of their ozone samples were measured relative to another specially prepared ozone sample assumed to provide the statistical distribution. This latter ozone sample was made at low pressure and the authors assumed that in this case "the essential features of ozone isotope effect are switched off" presumably implying no isotopic enrichment. However, as discussed earlier in section 3.2 this assumption is not correct and ozone made at low pressure cannot be considered as a reference to define enrichment relative to statistical distribution. Since the r values derived here are sensitively dependent on the two enrichments (symmetric and asymmetric) we believe that further TDLAS studies are required before one can compare them with the values derived here by relative fractionation method using high-precision mass spectrometric data.

[33] We can also compare our r values with that given in the recent study by *Liang et al.* [2006] who tried to reproduce the observed ozone isotope profiles of both ^{17}O and ^{18}O in stratosphere by considering two dominant processes: formation and photolysis. For comparison purpose, the profiles of enrichments of symmetric and asymmetric species using formation process alone (as given by *Liang et al.* [2006, Figure 7]) can be converted to r^{50} and r^{49} values as defined here and compared to our results. Such a comparison is given in Figure 10 showing variation of r^{50} and r^{49} as a function of enrichment in ^{18}O and ^{17}O respectively. First, we note that the r^{50} values of *Janssen* (as adopted here) agree well with the values of *Liang et al.*

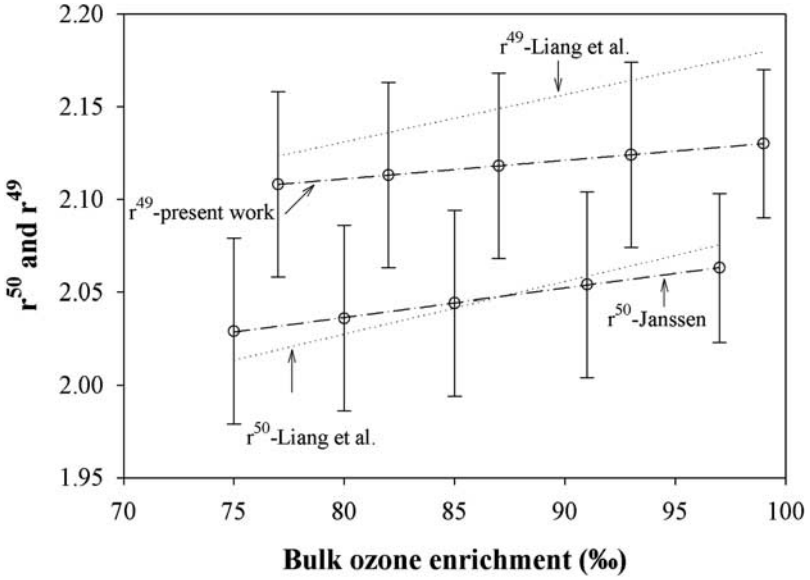

Figure 10. Comparison of values of r^{50} and r^{49} obtained from *Liang et al.* [2006] and *Janssen* [2005] with that obtained in the present study. The r^{49} values of Liang et al. are higher than those of present study by 0.01 to 0.05 (see Table 3).

[2006]. However, there is some disagreement in case of r^{49} between values of *Liang et al.* [2006] and our results (shown in Table 3 and Figure 10). In the Liang et al. case at bulk enrichment level of ~100‰ the value of ^{17}O enrichment in asymmetric species is slightly higher (by about 8‰) whereas that in symmetric species is slightly lower (by about 20‰) (see Table 3). This makes their r^{49} values slightly higher than our values (by 0.01 to 0.05). However, these differences may not be significant since they are within the error of our r^{49} values (~0.06). Additionally, it is to be noted that the values of r^{50} and r^{49} obtained by *Liang et al.* [2006] refer to their model calculation applicable to stratosphere (involving a large number of reactions) while our experiments deal with ozone made in the laboratory by Tesla discharge in pure molecular oxygen.

[34] A large number of publications dealing with ozone show that its isotopic composition depends on the temperature (T) and pressure (P) of oxygen gas during ozone formation. It is known [*Morton et al.*, 1990; *Janssen et al.*, 2003] that if the temperature increases the enrichment increases; similar effect occurs with decrease in pressure below the level of about 1000 torr [*Thiemens and Jackson*, 1988, 1990; *Morton et al.*, 1990; *Guenther et al.*, 1999]. It is possible that the P and T of the ozone forming zone will affect the internal distribution but our results show that the distribution probably depends only on the net enrichment since the UV data were obtained by varying P alone whereas the Tesla data were obtained by varying both P and T and they show the same pattern. However, we still do not know how UV dissociation of ozone influenced the $O(^1D)$ isotopic composition and how it varies with temperature. It is an important issue to be addressed in future studies for application to stratospheric ozone where both factors change significantly with increasing altitude and the formation is induced mainly by UV dissociation.

3.4. Application to Atmospheric Studies

[35] The intramolecular distribution of isotopes in ozone is of interest because of several reasons. In the atmosphere, the anomalous isotopic signature gets transferred from ozone to other oxygen containing trace gases, like CO_2, HNO_3, H_2SO_4, N_2O [*Gamo et al.*, 1989, 1995; *Yung et al.*, 1991, 1997; *Thiemens*, 1999; *Thiemens et al.*, 1995a, 1995b; *Thiemens*, 2006; *Lyons*, 2001; *Chakraborty and Bhattacharya*, 2003; *Johnston et al.*, 2000; *Lämmerzahl et al.*, 2002; *Brenninkmeijer et al.*, 2003; *Shaheen et al.*, 2007; *Liang et al.*, 2007; *McLinden et al.*, 2003; *Savarino et al.*, 2000, 2003; *Alexander et al.*, 2002; *Baroni et al.*, 2007; *Michalski et al.*, 2003; *Cliff and Thiemens*, 1997;

Table 3. A Comparison of r^{50} and r^{49} Values Obtained From *Liang et al.* [2006], *Janssen* [2005], and This Work[a]

Bulk Ozone Enrichment, ‰	r^{50}, *Liang et al.* [2006]	r^{50}, *Janssen* [2005]	r^{49}, *Liang et al.* [2006] (A)	r^{49}, This Work (B)	Difference (A − B)
75	2.015	2.029	2.118	2.106	0.012
80	2.028	2.036	2.129	2.111	0.018
85	2.039	2.044	2.145	2.116	0.029
91	2.056	2.054	2.158	2.122	0.036
97	2.078	2.063	2.174	2.128	0.046

[a]The total error in r^{50} and r^{49} is 0.05. The r^{49} values calculated from *Liang et al.* [2006] are slightly higher than that of this work (by 0.01 to 0.05).

Table 4. $\Delta^{17}O$ (Defined as $\delta^{17}O - 0.515 \times \delta^{18}O$) Values for Bulk, Terminal, and Central Positions[a]

	Ozone[b]		$\Delta^{17}O$ in Ozone		
Sample	$\delta_b^{18}O$	$\delta_b^{17}O$	Bulk	Terminal Position	Central Position
P-1	13.7	16.6	9.4	23.1	−17.9
P-2	18.3	21.7	12.2	24.0	−11.5
P-3	22.0	23.9	12.5	28.6	−19.8
P-4	33.6	30.4	12.9	28.5	−18.4
P-5	34.5	35.1	17.1	27.3	−3.2
P-6	40.8	37.8	16.5	32.7	−15.8
P-7[c]	43.1	40.5	18.1	29.9	−5.5
P-8	44.4	41.0	17.9	34.6	−15.5
P-9	46.9	44.1	19.6	36.8	−14.7
P-10	47.2	41.8	17.3	35.4	−19.0
P-11	49.3	45.1	19.4	33.5	−8.6
P-12	51.1	43.3	16.7	27.4	−4.7
P-13	51.3	43.4	16.7	26.8	−3.3
P-14	51.9	47.6	20.5	34.0	−6.3
P-15[c]	54.7	51.3	22.9	31.7	5.2
P-16	56.1	48.6	19.4	33.1	−8.0
P-17	59.0	53.0	22.4	34.0	−0.8
P-18	62.6	50.8	18.3	30.6	−6.4
P-19	67.4	63.7	28.7	46.1	−6.1
P-20	68.7	64.5	28.8	46.1	−5.9
P-21	69.1	63.9	27.9	46.1	−8.4
P-22	71.3	66.4	29.4	47.2	−6.3
P-23[c]	72.5	71.0	33.3	44.0	12.0
P-24	77.3	70.3	30.1	47.6	−4.9
P-25	78.0	70.5	29.9	46.6	−3.5
P-26[c]	81.4	76.9	34.6	48.5	6.8
P-27[c]	89.8	83.5	36.8	51.6	7.3
P-28[c]	91.8	88.1	40.4	54.0	13.2
P-29[c]	97.1	92.6	42.1	52.6	21.0
P-30[c]	101.8	87.2	34.3	47.2	8.4
P-31[c]	102.0	95.6	42.6	60.3	7.1
P-32[c]	102.4	96.3	43.0	54.8	19.3
P-33[c]	104.3	95.9	41.7	54.0	17.0
P-34[c]	104.7	98.2	43.7	56.1	19.0
P-35[c]	111.6	104.3	46.3	64.0	11.0
P-36[c]	112.8	102.0	43.3	58.5	13.0
P-37[c]	115.6	106.3	46.2	63.2	12.3
L-1	10.7	11.7	6.1	18.2	−18.0
L-2	20.7	21.7	10.6	23.2	−13.5
L-3	28.1	29.0	14.4	26.5	−9.7
L-4	39.4	40.4	19.9	31.9	−4.0
L-5	45.9	45.4	21.6	33.5	−2.4
L-6	52.3	51.6	24.4	36.2	0.9
L-7	53.1	51.3	23.6	35.8	−0.7
L-8	60.7	57.1	25.5	36.0	4.6
L-9	64.4	60.4	26.9	40.8	−1.0
L-10	76.4	70.4	30.7	44.3	3.5
L-11	83.9	75.4	31.8	45.8	3.8
L-12	84.1	76.6	32.9	46.1	6.3
L-13	86.4	76.8	31.9	42.2	11.1
L-14	98.2	84.5	33.5	47.1	6.2
L-15	106.2	91.8	36.6	51.7	6.3
1[d]	−9.5	−5.5	−0.6	2.1	−6.0
2[d]	−8.9	−4.4	0.2	1.1	−1.6
3[d]	−8.8	−4.9	−0.3	5.3	−11.4
4[d]	−8.2	−4.2	0.1	4.8	−9.5
5[d]	−7.5	−3.7	0.2	3.2	−5.7
6[d]	−6.3	−3.5	−0.2	7.5	−15.8
7[d]	−5.4	−3.3	−0.5	6.8	−14.9
8[d]	−4.6	−2.1	0.3	7.4	−14.0
9[d]	−3.7	−2.1	−0.1	8.5	−17.4

[a]The data show that the values of $\Delta^{17}O$ for the terminal position are higher than those for the central position.

[b]Enrichment of ^{18}O and ^{17}O in bulk ozone. The rejected data (P-38 to P-45) shown in Table 2 are not given.

[c]In these cases, ozone was made by UV dissociation of O_2.

[d]In these cases, nearly 100% of the initial oxygen was converted to ozone (zero-enriched).

Röckmann et al., 2001; *Kaiser et al.*, 2004; *Kaiser and Röckmann*, 2005; S. K. Bhattacharya et al., Mass independent signature in oxygen isotopic enrichment of stratospheric carbon dioxide, submitted to *Journal of Geophysical Research*, 2006]. The transfer can occur in two ways: via isotopic exchange with $O(^1D)$ produced from ozone by UV photolysis or by direct reaction with ozone. This subject is of great importance as anomalous isotopic enrichment in trace species provides tracers for studying stratospheric transport processes and/or tropospheric oxidation reaction pathways. In order to explain the mass-independent isotopic anomaly in molecules arising out of reaction or exchange with ozone, the isotopic composition of $O(^1D)$ and intramolecular isotope distribution in O_3 should be known. However, direct isotopic measurement of $O(^1D)$ is not yet possible because of its low concentration. It is, of course, clear that the isotopic composition of $O(^1D)$ should depend on (1) the intramolecular distribution of heavy oxygen isotope in ozone and (2) the relative photolysis rate coefficients of terminal and central position during ozone dissociation. As mentioned in the Introduction, regarding the latter point, an earlier theoretical study [*Sheppard and Walker*, 1983] indicated that in ozone dissociation by photons, it is quite probable that only one of the two terminal atoms is emitted since the probability of central atom emission is calculated to be less than 9%. All recent workers assumed that ozone normally dissociates by losing one terminal atom [*Brenninkmeijer et al.*, 2003; *Babikov et al.*, 2003; *Janssen*, 2005; *Cole and Boering*, 2006]. Under this assumption, the isotopic composition of $O(^1D)$ emitted by ozone dissociation can be estimated if the values of asymmetric/symmetric ratio, r^{50} and r^{49} are known along with the bulk enrichment in ozone. More generally, O_3 is a strong oxidant molecule that reacts directly with many trace species in the atmosphere, including nitrogen oxides, sulfur oxides, halogens and organic matter. During such oxidation reactions, oxygen atoms from the ozone are incorporated into the products, thereby transferring its anomalous isotope composition to the end product of oxidation. It is possible that even though photodissociation favors the ejection of a terminal atom, direct contact of ozone with molecules may result in partial abstraction of the central oxygen atom [*van den Ende et al.*, 1982; *van den Ende and Stolte*, 1984]. In either case, to establish an isotopic anomaly transfer budget, knowledge of the internal oxygen isotope distribution of O_3 is absolutely necessary.

[36] Determination of accurate values of r^{50} and r^{49} as a function of bulk enrichment in ozone is very important to study the enrichment transfer from ozone to CO_2 in stratosphere through exchange of $O(^1D)$ with normal CO_2. Stratospheric CO_2 is enriched in heavy isotopes with a $\Delta(\delta^{17}O)/\Delta(\delta^{18}O)$ slope ~1.7. This poses a problem since this slope value is radically different from that of the parent ozone reservoir (~0.85 with air O_2 as the origin [*Mauersberger et al.*, 2001]) which is responsible for the heavy isotope enrichment in CO_2. This issue has been successfully addressed in a recent paper by *Liang et al.* [2007] who showed that if the $O(^1D)$ atoms produced by ozone photolysis are obtained from the terminal position they would have the appropriate composition to generate the anomalous CO_2 due to the difference in internal distribution of ^{18}O and ^{17}O in ozone. In their calculations *Liang et al.*

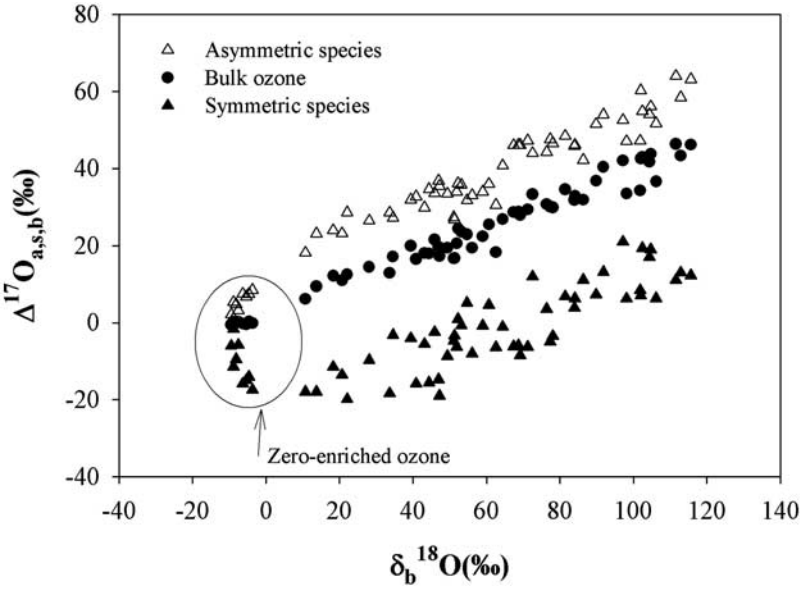

Figure 11. $\Delta^{17}O$ (defined as $\delta^{17}O - 0.515 \times \delta^{18}O$) values of asymmetric species, symmetric species and bulk ozone plotted against $\delta_b{}^{18}O$ (bulk) ozone. It is seen that asymmetric ozone species has significantly higher $\Delta^{17}O$ than that of symmetric species.

[2006, 2007] used the theoretical model of *Gao and Marcus* [2002] to determine the terminal position composition which was developed for one particular ozone enrichment level. The present experimental data provide the internal distribution for ^{17}O and supplement the earlier result for ^{18}O over a wide range of enrichment levels and thus act as valuable input for the Liang et al.-type model.

[37] Similarly, the enrichment transfer from ozone to atmospheric molecules like nitrate, water, ClO_x, CO_2, etc. depends not only on the level of the bulk enrichment but also on the internal distribution of ^{18}O and ^{17}O. The fractionation associated with chemical reactions or transport processes are known to be mass-dependent and their effect in isotope transfer can be ignored if one uses the $\Delta^{17}O$ (defined as $\delta^{17}O - 0.515 \times \delta^{18}O$) rather than $\delta^{18}O$ and $\delta^{17}O$. It is possible to calculate $\Delta^{17}O$ at terminal and central position in ozone only when both the internal distributions for ^{17}O and ^{18}O are known. Since our study provides this distribution, $\Delta^{17}O$ can be calculated for bulk, terminal and central positions in ozone (Table 4) and is shown in Figure 11. It is observed that $\Delta^{17}O$ for the terminal position is significantly higher than the central position and the bulk $\Delta^{17}O$. If the contribution from terminal and central positions of ozone during the reaction or dissociation is known then using appropriate mix of two $\Delta^{17}O$ values it would be possible to explain the oxygen anomaly in other species. For example, atmospheric nitrate possesses very high $\Delta^{17}O$ value (varies from 20 to 40‰) which possibly originates through NO_x oxidation by ozone [*Michalski et al.*, 2003]. To explain this variation they assumed that NO abstracts only the terminal atom of ozone to produce the NO_2. This assumption seems to be valid in case of photodissociation. As of now, our study strongly suggests that this assumption is also valid for $NO + O_3$ reaction, otherwise it would be difficult to generate such a high value of $\Delta^{17}O$ in nitrate. Nevertheless, this reaction is currently under study in our laboratory.

4. Conclusion

[38] There are earlier spectroscopic works (summarized by *Janssen* [2005]) dealing with intramolecular distribution in case of ^{18}O but for ^{17}O there is no clear result because of limited accuracy in laboratory spectroscopic data. We have investigated the internal distribution of ^{17}O isotope in ozone isotopomers using a new and simple idea of oxidation reaction of ozone with silver. Assuming that the oxidation process involves transfer of an O atom to silver from the terminal position of the triangular ozone molecule it is possible to deduce the distribution of the ^{17}O isotope inside the ozone molecule. In this method the heavy isotope ratios ($^{18}O/^{16}O$ and $^{17}O/^{16}O$) of silver oxide and ozone are used along with information on ^{18}O distribution in ozone (i.e., asymmetric/symmetric ratio in case of ^{18}O or r^{50}) to determine $r^{49} = [^{16}O^{16}O^{17}O]/[^{16}O^{17}O^{16}O]$. Using the compilation of *Janssen* [2005] on the internal distribution of ^{18}O in ozone molecule we derive the value of kinetic fractionation associated with silver oxidation and calculate the ratio of asymmetric to symmetric type of ozone isotopomers for ^{17}O species given by r^{49}. It is seen that r^{49} values increase from 2.030 to 2.145 with increase in bulk ^{17}O enrichment in ozone from 11.7‰ to 106.3‰ just as r^{50} values increase from 1.922 to 2.089 with increase in bulk ^{18}O enrichment over the same range. Moreover, r^{49} values are significantly higher than r^{50} values. For example, over bulk enrichment level up to ~100‰ the r^{49} values are higher than r^{50} values by 0.075 ± 0.026. The difference in r values is not large since the r^{50} and r^{49} values are not sensitive functions of enrichments but it is significant since it corresponds to a large change in enrichment values of the asymmetric and symmetric types of $^{17}O^{16}O_2$ and $^{18}O^{16}O_2$. The difference

Table A1. Estimation of Change in $\delta^{18}O$ of Ag_2O due to Effect of Catalytic Decomposition of Ozone[a]

	Chamber A				Chamber B					
		Ag_2O				Ag_2O				
Experiment	Exposure	Amount, μmol	$\delta^{18}O$, ‰	$\delta^{17}O$, ‰	Exposure	Amount, μmol	$\delta^{18}O$, ‰	$\delta^{17}O$, ‰	Difference in Ozone $\delta_b{}^{18}O$,[b] ‰	Effect of Catalysis (Difference in $\delta^{18}O$ of Ag_2O in A and B),[c] ‰
Blank[d]	ozone (48.0, 48.0)	21	***46.6***	58.9	ozone (48.0, 48.0)	18	***46.0***	57.7	0	***46.6*** **–** ***46.0*** = 0.6[e]
X[f]	#1 ozone X_1,[g] X_1: (29.6, 28.9)	7	***19.4***	38.3	#1 ozone X_1, X_1: (**29.6**, 28.9)	–	–	–	**29.6 – 22.0** = 7.6	***19.4*** **–** ***18.4*** = 1.0
X[f]					#2 ozone X_2, X_2: (**22.0**, 22.8)	12	***18.4***	37.4		
Y[h]	#1 ozone Y_1, Y_1: (26.0, 27.3)	–	–	–	#1 ozone Y_1, Y_1: (**26.0**, 27.3)	–	–	–		
Y[h]	#2 ozone Y_2, Y_2: (26.2, 28.6)	11	***16.7***	37.4	#2 ozone Y_2, Y_2: (**26.2**, 28.6)	–	–	–	**26.1 – 30.1** = –4	***16.7*** **–** ***16.4*** = 0.3
Y[h]					#3 ozone Y_3, Y_3: (**30.1**, 30.7)	16	***16.4***	38.1		

[a]Silver foils in chamber A and chamber B are exposed to ozone in different ways. Comparison of single and double exposure in chamber A and chamber B (experiment X), as well as double and triple exposure in A and B (experiment Y) respectively helps to quantify the net effect of catalysis. Numbers in bold and italics indicate the $\delta^{18}O$ values used for making comparison between the ozone samples used for reaction and catalysis and for determining the changes induced by catalysis in chamber B with reference to chamber A. The comparisons are shown in the last two columns.

[b]Difference in $\delta_b{}^{18}O$ values of two consecutive batch of ozone used for reaction with silver in chamber B.

[c]Difference in $\delta^{18}O$ values of Ag_2O after single and double exposure (in case of experiment X) and after double and triple exposure (in case of experiment Y).

[d]Same ozone was made to react with silver in chambers "A" and "B."

[e]The intrinsic chamber effect is 0.6‰.

[f]Silver in chamber A was exposed to ozone X_1 whereas silver in chamber B was exposed to ozone X_1 followed by ozone X_2. X_1 and X_2 are the isotopic compositions of ozone. The delta values of Ag_2O from both chambers were measured and compared.

[g]The isotopic composition expressed relative to the working gas ($\delta^{18}O$: 24.6, $\delta^{17}O$: 12.5 relative to V-SMOW). The amount of ozone (expressed in equivalent O_2) made in each case (X_1, X_2, Y_1, Y_2 and Y_3) was typically ~134 μmol; nearly half of this was made to react with silver in each chamber.

[h]Silver in chamber A was reacted with ozone Y_1 followed by Y_2 whereas silver in chamber B was exposed to ozone Y_1, Y_2 and Y_3 in succession.

reduces with increase in bulk ozone enrichment. We also show that the same difference is expected from known rate coefficient variation between these two species (at a particular bulk enrichment level) due to zero point energy difference. We do not find any significant difference in internal distribution between ozone samples generated by Tesla discharge and UV photolysis of oxygen.

[39] These results will be useful in calculating transfer of heavy isotopes from ozone to other atmospheric molecules during their interaction with ozone in stratosphere. For example, large $\Delta^{17}O$ values ($\Delta^{17}O = \delta^{17}O - 0.515 \times \delta^{18}O$) of atmospheric nitrate (~20 to 40‰) can now be explained as due to transfer of terminal atom from ozone which has higher $\Delta^{17}O$ than the bulk. The information on r^{50} and r^{49} values in ozone has also interesting application in deciphering reaction processes involving ozone. For example, in reactions involving direct contact of ozone [*Michalski et al.*, 2003; *Liang and Yung*, 2007] the position of the participating O atom is not always clear. If both positions are involved we need to know the proportion in which they react. Knowing the internal isotopic distribution of ozone and measuring the bulk isotopic transfer between O_3 and a given species one can get idea about the relative rate coefficients of these two positions which would elucidate many features of molecular reaction dynamics. In addition, we have also determined the distribution of heavy isotopes in zero-enriched ozone and find that the symmetrical isotopomers have relatively more heavy isotopes (for both ^{17}O and ^{18}O) than the asymmetrical ones in contrast to the case of enriched ozone; that is, the r values for ozone with negligible enrichment are always less than 2.00. This is opposite to the case of enriched ozone but can easily be explained by consideration of partition functions of these two isotopomers or from simple bond strength consideration.

Appendix A: Fractionation Associated With Catalytic Decomposition of Ozone by Silver Oxide

[40] A set of experiments were done to determine whether catalytic decomposition of oncoming stream of ozone by silver oxide can modify the oxygen isotopic composition of already formed silver oxide. In the experiment, few strips of silver foil were put in two identical chambers ("A" and "B") both of which were connected to another chamber where ozone was made by Tesla discharge of oxygen.

[41] To check whether silver reactions from both the chambers are identical, ozone with isotopic composition ($\delta_b{}^{18}O = 48.0$, $\delta_b{}^{17}O = 48.0$) was made to react with silver foils kept in chambers "A" and "B." After the reaction, silver oxides from the two chambers were heated separately and the released oxygen was collected for isotope measurements. It was observed that the $\delta^{18}O$ values of Ag_2O from chambers "A" and "B" are nearly same but not identical. The intrinsic chamber effect is ~0.6‰ (Table A1).

[42] The idea behind the control experiments was to expose silver in chamber "A" single (or double) time and chamber "B" double (or triple) times to ozone samples having nearly same amount and isotopic composition and then compare the isotopic compositions of Ag_2O produced in the two cases. Any difference in the δ values of Ag_2O from the two chambers will help in quantifying the net

effect of catalysis on Ag_2O composition. Two sets of experiments were done, designated as: X (chamber "A": single exposure and chamber "B": double exposure) and Y (chamber "A": double exposure and chamber "B": triple exposure) as described below.

A1. Experiment "X": (Chamber A, Single Exposure, and Chamber B, Double Exposure)

[43] Ozone with isotopic composition X_1 ($\delta_b^{18}O = 29.6$, $\delta_b^{17}O = 28.9$) was made and allowed to react with silver foils in chamber "A" and chamber "B." When the reaction was over, leftover oxygen was pumped out from both the chambers. Silver oxide from chamber "A" was heated separately to release the silver-bound oxygen which was collected in sample bottle containing molecular sieve for amount and isotope measurements. Silver in chamber "B" was again exposed to ozone having slightly different isotopic composition X_2 ($\delta_b^{18}O = 22.0$, $\delta_b^{17}O = 22.8$). After pumping out the leftover oxygen, silver oxide in chamber "B" was heated separately to release the oxygen (formed jointly in two exposures) for isotope measurements.

[44] The oxygen isotopic compositions of silver-bound oxygen from chamber "A" (7 μmol) and chamber "B" (12 μmol) were ($\delta^{18}O$, $\delta^{17}O$): (19.4, 38.3) and (18.4, 37.4) (see Table A1). This result demonstrates a decrease in $\delta^{18}O$ when second exposure is done by ozone having a lower δ value. When the difference in $\delta_b^{18}O$ values of the ozone used for the reaction in two cases ($X_1 - X_2$) is $\sim$7.6‰ the difference between $\delta^{18}O$ values in Ag_2O from chamber "A" and chamber "B" is $\sim$1.0‰.

A2. Experiment "Y": (Chamber A, Double Exposure, and Chamber B, Triple Exposure)

[45] In this case the silver foils in chamber "A" and chamber "B" were both exposed twice to two ozone samples having nearly same isotopic composition Y_1 (26.0, 27.3) and Y_2 (26.0, 28.6). After each reaction, leftover oxygen was pumped out. Then silver oxide from chamber "A" (double exposure) was heated and the isotopic composition of the released oxygen was measured. Next, silver in chamber "B" was again exposed to ozone having a slightly higher δ value Y_3 (30.1, 30.7). The leftover O_2 was pumped out and silver oxide was heated to release the oxygen. The isotopic composition of silver oxide from chamber "A" (11.4 μmol) and chamber "B" (16 μmol) were ($\delta^{18}O$, $\delta^{17}O$): (16.7, 37.4) and (16.4, 38.1) (see Table A1). This shows that when the difference in $\delta_b^{18}O$ of the ozone sample used for first two reactions is 4‰ the difference between the $\delta^{18}O$ values in Ag_2O from chamber "A" and chamber "B" is only 0.3‰.

[46] The above experiments show that when ozone used for a second phase of reaction plus catalysis differs from that used for the first phase there is a change in $\delta^{18}O$ of Ag_2O which depends on the isotope difference between the two ozone samples. When the difference is +7.6‰ (experiment X) the effect is +1‰ change. If the difference reduces to 4‰ (experiment Y) the effect goes down to approximately +0.3‰ which is not significant as the chamber difference itself is $\sim$0.6‰. This suggests that when catalysis is induced by ozone having very different composition from the one that made the silver oxide it is possible to have extra fractionation. In our experiments the ozone that flows in later may have enriched composition and cause secondary enrichment of the preformed silver oxide.

Appendix B: Estimation of the Values of r^{50} and r^{49} From Known Relative Rate Coefficients

B1. Estimation of r^{50} From Relative Rate Coefficients of ^{18}O Species

[47] We first evaluate the available rate coefficient data. As mentioned before, *Tuzson* [2005] tried to estimate the relative rate coefficients for ^{17}O and ^{18}O species using a new TDLAS technique. However, there is a large discrepancy for ^{18}O species between Tuzson's data and *Janssen* [2005] compilation. The reason for this difference is probably related to the choice of low-pressure ozone as statistical reference for isotope ratios. As stated by *Tuzson and Janssen* [2006], until the composition of the reference ozone is known with respect to a molecular oxygen standard this issue cannot be resolved. Here we have assumed that the relative rate coefficient values for ^{18}O species as given by *Janssen et al.* [2001] are true. For ^{17}O species, we have adopted the rate coefficient values from *Gao and Marcus* [2002] since their calculations reproduce the Janssen et al. values for ^{18}O accurately.

[48] *Janssen et al.* [2001] summarized the relative rate coefficients of reaction channels of several possible oxygen isotope combinations leading to ozone molecules at ambient pressure of 267 hPa corresponding to bulk ozone enrichment (in ^{18}O) of $\sim$128‰. The relevant equations (along with relative rate coefficients) which lead to formation of asymmetric and symmetric ozone species in this case are given below. The formation rate of OOO has a value of $k_1 = 6.0 \times 10^{-34}$ cm^6 s^{-1}.

(RB1) $^{16}O + {}^{16}O^{16}O \rightarrow {}^{16}O^{16}O^{16}O \qquad k_1 = 1.00$

For ^{18}O-containing species:

(RB2) $^{16}O + {}^{16}O^{18}O \rightarrow {}^{16}O^{16}O^{18}O \qquad k_2 = 1.45 \pm 0.04$

(RB3) $^{16}O + {}^{16}O^{18}O \rightarrow {}^{16}O^{18}O^{16}O \qquad k_3 = 1.08 \pm 0.01$

(RB4) $^{18}O + {}^{16}O^{16}O \rightarrow {}^{16}O^{16}O^{18}O \qquad k_4 = 0.92 \pm 0.04$

(RB5) $^{18}O + {}^{16}O^{16}O \rightarrow {}^{16}O^{18}O^{16}O \qquad k_5 = 0.006 \pm 0.005$

All the rate coefficient values are normalized to k_1. In reactions (RB2) and (RB3), ^{16}O atom collides with heteronuclear oxygen molecule $^{16}O^{18}O$ and leads to the formation of $^{16}O^{16}O^{18}O$ and $^{16}O^{18}O^{16}O$ respectively. The relative reaction probabilities for these two reactions are $k_2 = 1.45 \times k_1$ and $k_3 = 1.08 \times k_1$. The corresponding relative rate coefficients are obtained by dividing these numbers by two since there are two product channels. The values of rate coefficients (k_1 to k_5) for both asymmetric and symmetric ozone formation channels corresponding to reactions (RB1)–(RB5) are valid for enrichment level of 128.5‰ in ^{18}O; these are used here to first calculate the

enrichments in asymmetric and symmetric species of $^{18}O^{16}O_2$ and then determine the value of r^{50}.

[49] In a scrambled system, ozone is made by photolysis of molecular oxygen. By definition, $[^{16}O^{18}O]/[^{16}O^{16}O] = 2f$, where F is the $[^{18}O]/[^{16}O]$ atomic ratio. Molecular oxygen isotope ratio is taken as representative of statistical ratio 2f. If a statistical distribution of heavy oxygen isotope (^{18}O) in ozone is assumed then,

$$\left[^{16}O^{18}O^{16}O\right] + \left[^{18}O^{16}O^{16}O\right] / \left[^{16}O^{16}O^{16}O\right] 3f$$

The atomic oxygen generated during O_2 photolysis undergoes a fast isotopic exchange with O_2 which depletes the ^{16}O atom pool in ^{18}O ~75‰ [*Anderson et al.*, 1985]. Therefore the isotopic ratio $[^{18}O]/[^{16}O]$ of the O atom pool is less than F and we have, $[^{18}O]/[^{16}O] = 0.924f$.

[50] Following the definition given below, the bulk enrichment in ozone (in ‰) can be calculated as

$$\begin{aligned}
&\left(1 + \delta_b^{18}O/1000\right) \\
&= \frac{\left\{\frac{1}{2}(k_2 + k_3)[^{16}O][^{16}O^{18}O] + (k_4 + k_5)[^{18}O][^{16}O^{16}O]\right\}}{k_1[^{16}O][^{16}O^{16}O]} \Big/ 3f \\
&= \left\{1/2(k_2 + k_3)\left[^{16}O^{18}O\right]/\left[^{16}O^{16}O\right] + (k_4 + k_5)\left[^{18}O\right]\right. \\
&\quad \left./\left[^{16}O\right]\right\}/(3f \times k_1) \\
&= \{(k_2 + k_3) + (k_4 + k_5) \times 0.924\}/(3k_1) \\
&= 1.1285 \pm 0.019 \qquad \text{(B1)}
\end{aligned}$$

Using the rate coefficients given above we thus get, $\delta_b^{18}O = 128.5 \pm 19‰$.

[51] For calculating the enrichment in asymmetric ozone species, only those channels need to be considered which lead to the formation of asymmetric ozone.

$$\begin{aligned}
\left(1 + \delta_b^{18}O/1000\right) &= \frac{\left\{1/2(k_2)[^{16}O][^{16}O^{18}O] + (k_4)[^{16}O][^{16}O^{16}O]\right\}}{k_1[^{16}O][^{16}O^{16}O]} \\
&\quad \Big/ 2f \\
&= \{1/2(k_2)\left[^{16}O^{18}O\right]/\left[^{16}O^{16}O\right] + (k_4)\left[^{18}O\right] \\
&\quad \left./\left[^{16}O\right]\right\}/(2f \times k_1) \\
&= \{(k_2 + k_4) \times 0.924\}/(2k_1) \\
&= 1.150 \pm 0.027 \qquad \text{(B2)}
\end{aligned}$$

Therefore $\delta_a^{18}O = 150.0 \pm 27‰$.

[52] Similarly, the enrichment in symmetric ozone is calculated as,

$$\begin{aligned}
\left(1 + \delta_b^{18}O/1000\right) &= \frac{\left\{1/2(k_3)[^{16}O][^{16}O^{18}O] + (k_5)[^{18}O][^{16}O^{16}O]\right\}}{k_1[^{16}O][^{16}O^{16}O]} \\
&\quad \Big/ f \\
&= 1/2(k_3)\left[^{16}O^{18}O\right]/\left[^{16}O^{16}O\right] + (k_5)\left[^{18}O\right] \\
&\quad \left./\left[^{16}O\right]\right\}(f \times k_1) \\
&= \{(k_3 + k_5) \times 0.924\}/(k_1) \\
&= 1.0855 \pm 0.011 \qquad \text{(B3)}
\end{aligned}$$

$\delta_s^{18}O = 85.5 \pm 11‰$. Therefore the corresponding r value is:

$$r^{50} = 2\left(1 + 10^{-3} \times \delta_a^{18}O\right)/\left(1 + 10^{-3} \times \delta_s^{18}O\right) = 2.119 \pm 0.102$$

B2. Estimation of r^{49} From Relative Rate Coefficients of ^{17}O Species

[53] For ^{17}O-containging species, the relevant equations are given below.

(RB6) $^{16}O + ^{16}O^{17}O \rightarrow ^{16}O^{16}O^{17}O \quad k_6 = 1.36 \pm 0.05$

(RB7) $^{16}O + ^{16}O^{17}O \rightarrow ^{16}O^{17}O^{16}O \quad k_7 = 1.06 \pm 0.01$

(RB8) $^{17}O + ^{16}O^{16}O \rightarrow ^{16}O^{16}O^{17}O \quad k_8 = 0.98 \pm 0.05$

(RB9) $^{17}O + ^{16}O^{16}O \rightarrow ^{16}O^{17}O^{16}O \quad k_9 = 0.006 \pm 0.005$

The values of relative rate coefficients for (RB6), (RB7) and (RB9) are not available from *Janssen et al.* [2001]. Even though the rate coefficient k_8 for (RB8) is given there is an unknown contribution from other symmetric molecules. Therefore we need to estimate all of them from other considerations as described below.

[54] For reactions (RB6) and (RB7), we can use the argument of *Janssen et al.* [2001] relating change in zero point energy of the corresponding exchange reaction ($^{16}O + ^{16}O^{17}O \Longleftrightarrow {}^{17}O + {}^{16}O^{16}O$) with the relative reaction probability and use the same linear relation obtained for ^{18}O species, i.e., $k = [0.013 \times \Delta ZPE + 1.2]\, k_1$. In (RB6), the relevant zero point energy change is 11.7 cm^{-1} which corresponds to $k_6 = 1.35 \times k_1$. This value is close to the value 1.36 given by *Gao and Marcus* [2002] based on more detailed analysis. We adopted the Gao-Marcus value for our calculations.

[55] The value of rate coefficient k_7 of symmetric ozone formation channel was not measured. *Gao and Marcus* [2002] calculated this rate to be 1.02 at 300 K. If we consider the symmetric channel for ^{18}O, the value of k_3 calculated by *Gao and Marcus* [2002] is 1.04 in contrast to 1.08 measured by *Janssen et al.* [2001]. There is a discrepancy of 0.04 between the calculated and experimentally measured value. Applying the same discrepancy 0.04 as an additive correction the value of k_7 is taken to be 1.06. The average relative rate coefficient for the two asymmetric channels (k_6 and k_8) for the formation of $^{16}O^{16}O^{17}O$ considered together was derived by *Mauersberger et al.* [1999] to be 1.17. Since the relative rate coefficient k_6 is taken to be 1.36, the value of relative rate coefficient k_8 for other asymmetric channel should to be 0.98 ((1.36+0.98)/2 = 1.17). The value of k_9 was taken to be same as k_5.

[56] In a scrambled system,

$$\left[^{16}O^{17}O\right]/\left[^{16}O^{16}O\right] = 2g \text{ and } \left\{\left[^{16}O^{17}O^{16}O\right] + \left[^{17}O^{16}O^{16}O\right]\right\}/\left[^{16}O^{16}O^{16}O\right] = 3g$$

As argued before for ^{18}O species, the atomic oxygen generated during O_2 photolysis undergoes a fast isotopic

exchange with O_2 which depletes the O atom pool in ^{17}O by ~39‰ [*Anderson et al.*, 1985]. Therefore the isotopic ratio $^{17}O/^{16}O$ of the O atom pool is less than g and we have, $^{17}O/^{16}O = 0.961g$.

[57] Calculations similar to ^{18}O species (i.e., (B1), (B2) and (B3)) can be done for ^{17}O species to calculate the enrichment in asymmetric and symmetric ozone species and then to calculate r^{49}. These are given below.

$$\left(1+\delta_b^{17}O/1000\right) = \{(k_6+k_7)+(k_8+k_9)\times 0.961\}/3k_1 = 1.1225 \pm 0.023 \quad \text{(B4)}$$

$$\left(1+\delta_a^{17}O/1000\right) = \{k_6+k_8\times 0.961\}/(2k_1) = 1.1509 \pm 0.035 \quad \text{(B5)}$$

$$\left(1+\delta_s^{17}O/1000\right) = \{k_7+k_9\times 0.961\}/k_1 = 1.0658 \pm 0.011 \quad \text{(B6)}$$

These show that a bulk enrichment ($\delta_b^{17}O$) of 122.5‰ corresponds to an enrichment of 150.9‰ in $\delta_a^{17}O$ and 65.8 ‰ in $\delta_s^{17}O$. Using the above values of the bulk enrichment as well as that in asymmetric and symmetric species for ^{17}O the value of r^{49} is 2.160 ± 0.133 (at $\delta_b^{17}O$ ~122.5‰). If the enrichment is larger and equal to 128.5‰ (to equal that of ^{18}O) the r value would be slightly higher.

[58] Thus we see that at bulk enrichment level of ~120‰ the calculated value of r^{49} (2.160) is indeed more than calculated value of r^{50} (~2.119). From our experiment a slightly lower value of r^{49} (2.154) is obtained from a projection of the equation relating r^{49} with bulk enrichment (see Figure 8). As can be seen from the formulae (B2) and (B5) given above, the difference arises in large part because of ZPE effect on the exchange which favors ^{17}O relative to ^{18}O in the molecular oxygen resulting in lower enrichment in symmetric species for $^{17}O^{16}O_2$ than that of $^{18}O^{16}O_2$.

Appendix C: Estimation of Total Error in r^{49} Value

[59] There are three major sources of error in the above method. As described above, for each experiment we have used the value of r^{50}, derived from *Janssen*'s [2005] equation corresponding to the observed ^{18}O enrichment, to determine the fractionation factor for ^{18}O first and then that of ^{17}O. Next, we calculate the value of r^{49}. So any error associated with r^{50} measurement gets reflected in r^{49} values. Since a small change in r values affect the δ values significantly we prefer to give three digits after the decimal point to circumvent the grounding off effect.

[60] A second source of error in r^{49} arises because of variation or spread in $\delta^{18}O$ and $\delta^{17}O$ values of Ag_2O. At a fixed ozone composition, we expect a constant δ value of Ag_2O. However, experimentally, there is variation in both $\delta^{18}O$ and $\delta^{17}O$ values of Ag_2O as evident from Figure 2. This variation is possibly due to the kinetics associated with the ozone-silver reaction such as diffusion of ozone molecules during streaming in the silver chamber, variable kinetic fractionation associated with the rapid formation of silver oxide and the effect of catalysis. Since the Ag_2O-delta values are used to calculate the fractionation factor, any spread in $\delta^{18}O$ and $\delta^{17}O$ values of Ag_2O will introduce uncertainty in values of α^{18} and α^{17} and finally in r^{49} values. Considering above facts, the total error in r^{49} was estimated as follows:

[61] The fractionation factor for ^{18}O was calculated using the measured value of Ag_2O and $\delta^{18}O$ (terminal) calculated from Janssen's equation.

$$\alpha^{18} = R^{18}(Ag_2O)/R_a^{18}(O_3) = \left(10^3+\delta^{18}O(Ag_2O)\right)/\left(10^3+\delta_a^{18}O\right)$$

$$\alpha^{17} = \left(\alpha^{18}\right)^{\lambda} = \left(10^3+\delta^{17}O(Ag_2O)\right)/\left(10^3+\delta_a^{17}O\right),$$

where the value of λ is taken to be 0.515 as applicable for many kinetic processes.

[62] Simplifying we get,

$$\left(10^3+\delta_a^{17}O\right) = \left[\left(10^3+\delta^{17}O(Ag_2O)\right)/\left(10^3+\delta^{18}O(Ag_2O)\right)^{\lambda}\right] \times \left(10^3+\delta_a^{18}O\right)\lambda$$

[63] Taking log of both sides,

$$\ln\left(10^3+\delta_a^{17}O\right) = \ln\left(10^3+\delta^{17}O(Ag_2O)\right) - \lambda\ln\left(10^3+\delta^{18}O(Ag_2O)\right) + \lambda\ln\left(10^3+\delta_a^{18}O\right)$$

[64] Differentiating and casting in standard error-equation format,

$$\left(\frac{\Delta\delta_a^{17}O}{10^3+\delta_a^{17}O}\right)^2 = \left(\frac{\Delta\delta_a^{17}O(Ag_2O)}{10^3+\delta_a^{17}O(Ag_2O)}\right)^2 + \lambda^2\left(\frac{\Delta\delta^{18}O(Ag_2O)}{10^3+\delta^{18}O(Ag_2O)}\right)^2 + \lambda^2\left(\frac{\Delta\delta_a^{18}O(Ag_2O)}{10^3+\delta^{18}O(Ag_2O)}\right)^2$$

[65] Using this equation the error in $\delta_a^{17}O$ (i.e., $\Delta\delta_a^{17}O$) was calculated. The error in $\delta_s^{17}O$ and in r^{49} was calculated as follows (see equations (3) and (5)):

$$\left(\Delta\delta_s^{17}O\right)^2 = \left(3\times\Delta\delta_b^{17}O\right)^2 + \left(2\times\Delta\delta_a^{17}O\right)^2$$

and

$$\left(\frac{\Delta r^{49}}{r^{49}}\right)^2 = \left(\frac{2\times\Delta\delta_a^{17}O}{10^3+\delta_a^{17}O}\right)^2 + \left(\frac{\Delta\delta_s^{17}O}{10^3+\delta_s^{17}O}\right)^2$$

The calculated errors are given in Table C1 which shows that error associated with r^{49} values varies from 0.040 to 0.056 corresponding to errors in r^{50} from 0.03 to 0.08 (as given by Janssen). The mean difference between r^{49} and r^{50} values is 0.075 with a standard deviation of 0.026 (Table C1) which shows that r^{49} values are significantly higher than r^{50} values.

Table C1. Estimated Total Error in r^{49} Values[a]

Sample	$\delta_a{}^{18}O$	Error in $\delta_a{}^{18}O$	r^{50}	Total Error	Error in $\delta_a{}^{17}O$	Error in $\delta_s{}^{17}O$	r^{49}	Total Error in r^{49} (σ)	Difference $r^{49} - r^{50}$
P-1	1.1	14.0	1.927	0.08	9.8	20.6	2.043	0.056	0.115
P-2	7.2	14.0	1.936	0.08	9.8	20.6	2.036	0.056	0.100
P-3	12.1	13.0	1.943	0.07	9.4	19.8	2.066	0.054	0.123
P-4	27.3	13.0	1.964	0.07	9.4	19.7	2.074	0.054	0.110
P-5	28.5	13.0	1.965	0.07	9.4	19.8	2.041	0.053	0.076
P-6	36.7	11.0	1.976	0.07	8.7	18.4	2.083	0.050	0.107
P-7	39.6	11.0	1.980	0.07	8.7	18.3	2.059	0.049	0.079
P-8	41.3	11.0	1.983	0.07	8.7	18.4	2.090	0.050	0.107
P-9	44.6	11.0	1.986	0.06	8.7	18.4	2.094	0.050	0.108
P-10	44.9	11.0	1.987	0.06	8.7	18.3	2.101	0.050	0.114
P-11	47.7	11.0	1.991	0.06	8.7	18.4	2.078	0.049	0.087
P-12	50.0	11.0	1.994	0.06	8.7	18.4	2.059	0.049	0.066
P-13	50.2	11.0	1.994	0.06	8.7	18.4	2.055	0.049	0.062
P-14	51.1	11.0	1.995	0.06	8.7	18.4	2.076	0.049	0.081
P-15	54.6	11.0	1.999	0.06	8.7	18.3	2.051	0.048	0.052
P-16	56.4	11.0	2.002	0.06	8.7	18.4	2.082	0.049	0.080
P-17	60.1	10.0	2.006	0.06	8.3	17.7	2.071	0.047	0.064
P-18	64.7	10.0	2.012	0.06	8.3	17.7	2.079	0.047	0.067
P-19	70.9	10.0	2.020	0.06	8.3	17.7	2.113	0.047	0.093
P-20	72.6	9.0	2.022	0.05	8.0	17.1	2.113	0.046	0.091
P-21	73.1	9.0	2.022	0.05	8.0	17.1	2.119	0.046	0.096
P-22	75.8	9.0	2.026	0.05	8.0	17.1	2.118	0.045	0.092
P-23	77.5	9.0	2.028	0.05	8.0	17.1	2.076	0.044	0.048
P-24	83.5	9.0	2.035	0.05	8.0	17.1	2.121	0.045	0.086
P-25	84.5	9.0	2.037	0.05	8.0	17.1	2.117	0.045	0.080
P-26	88.7	8.0	2.041	0.05	7.7	16.5	2.102	0.043	0.061
P-27	99.4	7.0	2.054	0.04	7.4	16.0	2.113	0.041	0.060
P-28	101.9	7.0	2.057	0.04	7.5	16.1	2.108	0.041	0.051
P-29	108.6	7.0	2.064	0.04	7.5	16.1	2.093	0.041	0.029
P-30	114.5	7.0	2.071	0.04	7.5	16.1	2.112	0.041	0.041
P-31	114.7	7.0	2.071	0.04	7.4	16.0	2.139	0.041	0.069
P-32	115.2	7.0	2.071	0.04	7.5	16.1	2.105	0.041	0.033
P-33	117.6	7.0	2.074	0.04	7.5	16.1	2.109	0.041	0.035
P-34	118.1	7.0	2.075	0.04	7.5	16.1	2.110	0.041	0.035
P-35	126.6	6.0	2.084	0.03	7.2	15.6	2.145	0.040	0.061
P-36	128.2	6.0	2.085	0.03	7.2	15.7	2.132	0.040	0.046
P-37	131.7	6.0	2.089	0.03	7.2	15.7	2.144	0.040	0.055
P-38	3.6	14.0	1.931	0.08	9.8	19.6	2.054	0.056	0.123
P-39	17.7	13.0	1.951	0.08	9.4	18.9	1.997	0.052	0.046
P-40	59.0	11.0	2.005	0.06	8.7	17.4	2.085	0.049	0.080
P-41	63.6	11.0	2.011	0.06	8.7	17.4	2.062	0.048	0.051
P-42	84.5	9.0	2.036	0.05	8.1	16.1	2.050	0.044	0.014
P-43	112.7	7.0	2.069	0.04	7.5	15.0	2.086	0.041	0.017
P-44	118.1	7.0	2.074	0.04	7.5	15.0	2.081	0.041	0.007
L-1	−2.8	14.0	1.922	0.08	9.8	20.5	2.030	0.056	0.108
L-2	10.3	14.0	1.940	0.07	9.8	20.5	2.041	0.056	0.100
L-3	20.0	13.0	1.953	0.07	9.4	19.8	2.046	0.053	0.093
L-4	34.8	11.0	1.974	0.07	8.7	18.4	2.056	0.049	0.083
L-5	43.2	11.0	1.985	0.07	8.7	18.4	2.062	0.049	0.077
L-6	51.5	11.0	1.995	0.06	8.7	18.4	2.066	0.049	0.071
L-7	52.6	11.0	1.997	0.06	8.7	18.4	2.069	0.049	0.072
L-8	62.3	10.0	2.010	0.06	8.3	17.7	2.066	0.046	0.056
L-9	67.1	10.0	2.016	0.06	8.3	17.7	2.090	0.047	0.074
L-10	82.4	9.0	2.034	0.05	8.0	17.1	2.097	0.045	0.063
L-11	91.9	8.0	2.045	0.05	7.7	16.6	2.105	0.043	0.060
L-12	92.1	8.0	2.044	0.05	7.7	16.6	2.100	0.043	0.056
L-13	95.0	8.0	2.049	0.05	7.7	16.5	2.085	0.042	0.037
L-14	109.9	7.0	2.065	0.04	7.5	16.1	2.113	0.042	0.048
L-15	120.0	6.0	2.077	0.03	7.2	15.6	2.128	0.040	0.051
Mean									0.075
Standard deviation									0.026

[a]Total errors in $\delta_a{}^{18}$ and r^{50} are given as reported by *Janssen* [2005]. The values of r^{49} were calculated using Ag_2O delta values (see text). Total error (σ) in r^{49} is obtained after propagating the $\delta_a{}^{18}$ error as reported by Janssen and variation observed in $\delta^{18}O$ and $\delta^{17}O$ values of silver-bound oxygen (Ag_2O) through the calculations. The error associated with r^{49} values varies from 0.040 to 0.056. The mean of the difference between r^{49} and r^{50} is 0.075 and the standard deviation of the mean is 0.026.

[66] **Acknowledgments.** We are grateful to the Indo-French Centre for Promotion of Advanced Research for financial and other support to carry out this work in PRL, India, and LGGE, France. We are also indebted to PRL and LGGE authorities for their support in this program. The silver foil as a good candidate for reaction with ozone was suggested by S. Krishnaswami of PRL.

References

Abbas, M. M., J. Guo, B. Carli, F. Mencaraglia, M. Carlotti, and I. G. Nolt (1987), Heavy ozone distribution in the stratosphere from far-infrared observation, *J. Geophys. Res.*, *92*, 13,231–13,239.

Alexander, B., J. Savarino, N. I. Barkov, R. J. Delmas, and M. H. Thiemens (2002), Climate driven changes in the oxidation pathways of atmospheric sulfur, *Geophys. Res. Lett.*, *29*(14), 1685, doi:10.1029/2002GL014879.

Anderson, S. M., F. S. Klein, and F. Kaufman (1985), Kinetics of the isotope exchange reaction of ^{18}O with NO and O_2 at 298 K, *J. Chem. Phys.*, *83*(4), 1648–1656.

Anderson, S. M., J. Morton, and K. Mauersberger (1989), Laboratory measurements of ozone isotopomers by tunable diode-laser absorption spectroscopy, *Chem. Phys. Lett.*, *156*(2–3), 175–180.

Anderson, S. M., D. Hulsebusch, and K. Mauersberger (1997), Surprising rate coefficient for four isotopic variants of $O + O_2 + M$, *J. Chem. Phys.*, *107*(14), 5385–5392.

Babikov, D., B. K. Kendrick, R. B. Walker, R. T. Pack, P. Fleurat-Lesard, and R. Schinke (2003), Formation of ozone: Metastable states and anomalous isotope effect, *J. Chem. Phys.*, *119*(5), 2577–2589.

Bains-Sahota, S. K., and M. H. Thiemens (1987), Mass-independent oxygen isotopic fractionation in a microwave plasma, *J. Phys. Chem.*, *91*(16), 4370–4374.

Baroni, M., M. H. Thiemens, R. J. Delmas, and J. Savarino (2007), Mass-independent sulfur isotopic compositions in stratospheric volcanic eruptions, *Science*, *315*, 84–87.

Bhattacharya, S. K., and M. H. Thiemens (1989), New evidence for symmetry dependent isotope effects: O+CO reaction, *Z. Naturforsch.*, *44a*, 435–444.

Bhattacharya, S. K., S. Chakraborty, J. Savarino, and M. H. Thiemens (2002), Low-pressure dependency of the isotopic enrichment in ozone: Stratospheric implications, *J. Geophys. Res.*, *107*(D23), 4675, doi:10.1029/2002JD002508.

Bigeleisen, J., and M. Wolfsberg (1958), Theoretical and experimental aspects of isotope effects in chemical kinetics, *Adv. Chem. Phys.*, *1*, 15–76.

Brenninkmeijer, C. A. M., C. Janssen, J. Kaiser, T. Röckmann, T. S. Rhee, and S. S. Assonov (2003), Isotope effects in the chemistry of atmospheric trace compounds, *Chem. Rev.*, *103*, 5125–5161.

Chakraborty, S., and S. K. Bhattacharya (2003), Experimental investigation of oxygen isotope exchange between CO_2 and O (^1D) and its relevance to the stratosphere, *J. Geophys. Res.*, *108*(D23), 4724, doi:10.1029/2002JD002915.

Cliff, S. S., and M. H. Thiemens (1997), The $^{18}O/^{16}O$ and $^{17}O/^{16}O$ ratios in nitrous oxide: A mass independent anomaly, *Science*, *278*(5344), 1774–1776.

Cole, A. S., and K. A. Boering (2006), Mass-independent and non-mass-dependent isotope effects in ozone photolysis: Resolving theory and experiments, *J. Chem. Phys.*, *125*, 184,301.

Dole, M., G. A. Lane, D. P. Rudd, and D. A. Zaukelies (1954), Isotopic composition of atmospheric oxygen and nitrogen, *Geochim. Cosmochim. Acta*, *6*, 65–78.

Gamo, T., M. Tsutsumi, H. Sakai, T. Nakazawa, M. Tanaka, H. Honda, H. Kubo, and T. Itoh (1989), Carbon and oxygen isotopic ratios of carbon dioxide of a stratospheric profile over Japan, *Tellus, Ser. B*, *41*, 127–133.

Gamo, T., M. Tsutsumi, H. Skai, T. Nakazawa, T. Matchida, H. Honda, and T. Itoh (1995), Long term monitoring of carbon and oxygen isotope ratios of stratos pheric CO_2 over Japan, *Geophys. Res. Lett.*, *22*, 397–400.

Gao, Y. Q., and R. A. Marcus (2001), Strange and unconventional isotope effects in ozone formation, *Science*, *293*, 259–263.

Gao, Y. Q., and R. A. Marcus (2002), On the theory of the strange and unconventional isotopic effects in ozone formation, *J. Chem. Phys.*, *116*(1), 137–154.

Guenther, J., B. Erbacher, D. Krankowsky, and K. Mauersberger (1999), Pressure dependence of two relative ozone formation rate coefficients, *Chem. Phys. Lett.*, *306*(5–6), 209–213.

Hathorn, B. C., and R. A. Marcus (1999), An intramolecular theory of the mass-independent isotope effect for ozone I, *J. Chem. Phys.*, *111*(9), 4087–4100.

Hathorn, B. C., and R. A. Marcus (2000), An intramolecular theory of the mass-independent isotope effect for ozone. II. Numerical implementation at low pressures using a loose transition state, *J. Chem. Phys.*, *113*(21), 9497–9509.

Heidenreich, J. E., III, and M. H. Thiemens (1985), A non-mass dependent oxygen isotope effect in the production of ozone from molecular oxygen: The role of molecular symmetry in isotope chemistry, *J. Chem. Phys.*, *84*(4), 2129–2136.

Irion, F. W., M. R. Gunson, C. P. Rinsland, Y. L. Yung, M. C. Abrams, A. Y. Chang, and A. Goldman (1996), Heavy ozone enrichments from ATMOS infrared solar spectra, *Geophys. Res. Lett.*, *23*(17), 2377–2380.

Janssen, C. (2005), Intramolecular isotope distribution in heavy ozone ($^{16}O^{18}O^{16}O$ and $^{16}O^{16}O^{18}O$), *J. Geophys. Res.*, *110*, D08308, doi:10.1029/2004JD005479.

Janssen, C., and B. Tuzson (2006), A diode laser spectrometer for symmetry selective detection of ozone isotopomers, *Appl. Phys. B*, *82*, 487–494.

Janssen, C., J. Guenther, D. Krankowsky, and K. Mauersberger (1999), Relative formation rates of $^{50}O_3$ and $^{52}O_3$ in ^{16}O-^{18}O mixtures, *J. Chem. Phys.*, *111*(16), 7179–7182.

Janssen, C., J. Guenther, K. Mauersberger, and D. Krankowsky (2001), Kinetic origin of the ozone isotope effect: A critical analysis of enrichments and rate coefficients, *Phys. Chem. Chem. Phys.*, *3*(21), 4718–4721.

Janssen, C., J. Guenther, D. Krankowsky, and K. Mauersberger (2003), Temperature dependence of ozone rate coefficients and isotopologue fractionation in O-16-O-18 oxygen mixtures, *Chem. Phys. Lett.*, *367*(1–2), 34–38.

Johnston, J. C., and M. H. Thiemens (1997), The isotopic composition of tropospheric ozone in three environments, *J. Geophys. Res.*, *102*(D21), 25,395–25,404.

Johnston, J. C., T. Röckmann, and C. A. M. Brenninkmeijer (2000), CO2 + O (1D) isotopic exchange: Laboratory and modeling studies, *J. Geophys. Res.*, *105*, 15,213–15,229.

Kaiser, J., and T. Röckmann (2005), Absence of isotope exchange in the reaction of $N_2O + O$ (^1D) and the global $\Delta^{17}O$ budget of nitrous oxide, *Geophys. Res. Lett.*, *32*, L15808, doi:10.1029/2005GL023199.

Kaiser, J., et al. (2004), Contribution of mass-dependent fractionation to the oxygen isotope anomaly of atmospheric nitrous oxide, *J. Geophys. Res.*, *109*, D03305, doi:10.1029/2003JD004088.

Krankowsky, D., F. Bartecki, G. G. Klees, K. Mauersberger, K. Schellenbach, and J. Stehr (1995), Measurement of heavy isotope enrichment in tropospheric ozone, *Geophys. Res. Lett.*, *22*(13), 1713–1716.

Lämmerzahl, P., T. Röckmann, C. A. M. Brenninkmeijer, D. Krankowsky, and K. Mauersberger (2002), Oxygen isotope composition of stratospheric carbon dioxide, *Geophys. Res. Lett.*, *29*(12), 1582, doi:10.1029/2001GL014343.

Larsen, N. W., and T. Pedersen (1994), Microwave spectroscopy of isotopic cyclobutene ozonide as a means of quantification of ozone isotopomers, *J. Mol. Spectrosc.*, *166*(2), 372–382.

Larsen, R. W., N. W. Larsen, F. M. Nicolaisen, G. O. Sorensen, and J. A. Beukes (2000), Measurements of ^{18}O-enriched ozone isotopomer abundances using high-resolution Fourier transform far-IR spectroscopy, *J. Mol. Spectrosc.*, *200*(2), 235–247.

Liang, M.-C., F. W. Irion, J. D. Weibel, C. E. Miller, G. A. Blake, and Y. L. Yung (2006), Isotopic composition of stratospheric ozone, *J. Geophys. Res.*, *111*, D02302, doi:10.1029/2005JD006342.

Liang, M. C., G. A. Blake, B. R. Lewis, and Y. L. Yung (2007), Oxygen isotopic composition of carbon dioxide in the middle atmosphere, *Proc. Natl. Acad. Sci. U. S. A.*, *104*, 21–25, doi:10.1073/pnas.0610009104.

Liang, M. L., and Y. L. Yung (2007), Sources of the oxygen isotopic anomaly in atmospheric N_2O, *J. Geophys. Res.*, *112*, D13307, doi:10.1029/2006JD007876.

Lyons, J. R. (2001), Transfer of mass-independent fractionation in ozone to other oxygen-containing radicals in the atmosphere, *Geophys. Res. Lett.*, *28*(17), 3231–3234.

Mauersberger, K. (1987), Ozone measurements in the stratosphere, *Geophys. Res. Lett.*, *14*(1), 80–83.

Mauersberger, K., B. Erbacher, D. Krankowsky, J. Gunther, and R. Nickel (1999), Ozone isotope enrichment: isotopomer-specific rate coefficients, *Science*, *283*, 370–372.

Mauersberger, K., P. Lämmerzahl, and D. Krankowsky (2001), Stratospheric ozone isotope enrichments: Revisited, *Geophys. Res. Lett.*, *28*(16), 3155–3158.

McLinden, C. A., M. J. Prather, and M. S. Johnson (2003), Global modeling of the isotope analogues of N_2O: Stratospheric distributions, budgets, and the ^{17}O-^{18}O mass-independent anomaly, *J. Geophys. Res.*, *108*(D8), 4233, doi:10.1029/2002JD002560.

Meier, A., and J. Notholt (1996), Determination of the isotopic abundances of heavy O_3 as observed in arctic ground based FTIR spectra, *Geophys. Res. Lett.*, *23*, 551–554.

Michalski, G., Z. Scott, M. Kabiling, and M. H. Thiemens (2003), First measurements and modelling of $\Delta^{17}O$ in atmospheric nitrate, *Geophys. Res. Lett.*, *30*(16), 1870, doi:10.1029/2003GL017015.

Morton, J., J. Barnes, B. Schueler, and K. Mauersberger (1990), Laboratory studies of heavy ozone, *J. Geophys. Res.*, *95*(D1), 901–907.

Pandey, A., and S. K. Bhattacharya (2006), Anomalous oxygen isotope enrichment in CO_2 produced from O+CO: Estimates based on experimental results and model predictions, *J. Chem. Phys.*, *124*, 234,301, doi:10.1063/1.2206584.

Rinsland, C. P., V. M. Devi, J. M. Flaud, C. Camy-Peyret, M. A. Smith, and G. M. Stokes (1985), Identification of ^{18}O-isotope lines of ozone in

infrared ground based solar absorption spectra, *J. Geophys. Res.*, *90*, 10,719–10,725.

Röckmann, T., J. Kaiser, J. N. Crowley, C. A. M. Brennenkmeijer, and P. J. Crutzen (2001), The origin of the anomalous or "mass-independent" oxygen isotope fractionation in tropospheric N_2O, *Geophys. Res. Lett.*, *28*(3), 503–506.

Savarino, J., C. W. Lee, and M. H. Thiemens (2000), Laboratory oxygen isotopic study of sulfur (IV) oxidation: Origin of the mass independent oxygen isotopic anomaly in atmospheric sulfates and other sulfate mineral deposits, *J. Geophys. Res.*, *105*(D23), 29,079–29,089.

Savarino, J., S. Bekki, J. Cole-Dai, and M. H. Thiemens (2003), Evidence from sulfate mass independent oxygen isotopic compositions of dramatic changes in atmospheric oxidation following massive volcanic eruptions, *J. Geophys. Res.*, *108*(D21), 4671, doi:10.1029/2003JD003737.

Schueler, B., J. Morton, and K. Mauersberger (1990), Measurements of isotopic abundances in collected stratospheric ozone samples, *Geophys. Res. Lett.*, *17*, 1295–1298.

Shaheen, R., C. Janssen, and T. Rockmann (2007), Investigation of the photochemical isotope equilibrium between O_2, CO_2 and O_3, *Atmos. Chem. Phys.*, *7*, 495–509.

Sheppard, M. G., and R. B. Walker (1983), Wigner method studies of ozone photo-dissociation, *J. Chem. Phys.*, *78*(12), 7191–7199.

Thiemens, M. H. (1999), Mass-independent isotope effects in planetary atmospheres and the early solar system, *Science*, *283*, 341–345.

Thiemens, M. H. (2006), History and applications of mass-independent isotope effects, *Annu. Rev. Earth. Planet. Sci.*, *34*, 217–262.

Thiemens, M. H., and J. E. Heidenreich III (1983), The mass-independent fractionation of oxygen: A novel isotope effect and its possible cosmochemical implications, *Science*, *219*, 1073–1075.

Thiemens, M. H., and T. Jackson (1987), Production of isotopically heavy ozone by ultraviolet light photolysis of O_2, *Geophys. Res. Lett.*, *14*, 624–627.

Thiemens, M. H., and T. Jackson (1988), New experimental evidence for the mechanism for production of isotopically heavy O_3, *Geophys. Res. Lett.*, *15*(7), 639–642.

Thiemens, M. H., and T. Jackson (1990), Pressure dependency for heavy isotope enhancement in ozone formation, *Geophys. Res. Lett.*, *17*(6), 717–719.

Thiemens, M. H., T. Jackson, E. C. Zipf, P. W. Erdman, and C. van Egmond (1995a), Carbon dioxide and oxygen isotope anomalies in the mesosphere and stratosphere, *Science*, *270*, 969–972.

Thiemens, M. H., T. Jackson, and C. A. M. Brenninkmeijer (1995b), Observation of a mass independent oxygen isotopic composition in terrestrial stratospheric CO_2, the link to ozone chemistry and the possible occurrence in the Martian atmosphere, *Geophys. Res. Lett.*, *22*, 255–257.

Tuzson, B. (2005), Symmetry specific study of ozone isotopomer formation, dissertation, Univ. of Heidelberg, Heidelberg, Germany. (Available at http://www.ub.uni-heidelberg.de/archiv/5523)

Tuzson, B., and C. Janssen (2006), Unambiguous identification of ^{17}O containing ozone isotopomers for symmetry selective detection, *Isotopes Environ. Health Stud.*, *42*, 67–75.

van den Ende, D., and S. Stolte (1984), The influence of the orientation of the NO molecule upon the chemiluminescent reaction $NO + O_3 \rightarrow NO_2^* + O_2$, *Chem. Phys.*, *89*, 121–129.

van den Ende, D., S. Stolte, J. B. Cross, G. H. Kwei, and J. J. Valentini (1982), Evidence for two different transition states in the reaction of $NO + O_3 \rightarrow NO_2 + O_2$, *J. Chem. Phys.*, *77*(4), 2206–2208.

Waterhouse, G. I. N., G. A. Bowmaker, and J. B. Metson (2001), Oxidation of a polycrystalline silver foil by reaction with ozone, *Appl. Surf. Sci.*, *183*(3–4), 191–204.

Waterhouse, G. I. N., G. A. Bowmaker, and J. B. Metson (2002), Interaction of a polycrystalline silver powder with ozone, *Surf. Interface Anal.*, *33*(5), 401–409.

Wen, J., and M. H. Thiemens (1993), Multi-isotope study of the O (^1D)+CO_2 exchange and stratospheric consequences, *J. Geophys. Res.*, *98*(D7), 12,801–12,808.

Yung, Y. L., W. B. DeMore, and J. P. Pinto (1991), Isotopic exchange between carbon dioxide and ozone via O (^1D) in the stratosphere, *Geophys. Res. Lett.*, *18*(1), 13–16.

Yung, Y. L., A. Y. T. Lee, F. W. Irion, W. B. DeMore, and J. Wen (1997), Carbon dioxide in the atmosphere: Isotopic exchange with ozone and its use as a tracer in the middle atmosphere, *J. Geophys.Res.*, *102*(D9), 10,857–10,866.

S. K. Bhattacharya and A. Pandey, Physical Research Laboratory, Navrangpura, Ahmedabad 380009, India. (bhatta@prl.res.in)

J. Savarino, Laboratoire de Glaciologie et Géophysique de l'Environnement, Centre National de la Recherche Scientifique, Université Joseph Fourier-Grenoble, 54 rue Molière BP96, Saint Martin d'Heres F-38402, France.